

FIELD DEPENDENCE OF SPIN-LATTICE RELAXATION TIMES

Field Dependence of Spin-Lattice
Relaxation Times in Cr^{3+} .

by

Nicholas Rumin MSc.

A thesis submitted to the Faculty of
Graduate Studies and Research in partial
fulfilment of the requirements for the
degree of Doctor of Philosophy.

Eaton Electronics Research Laboratory and
The Department of Electrical Engineering,
McGill University,
Montreal.

August 1965.

ABSTRACT.

The changes in spin-lattice relaxation time with the magnitude and orientation of the dc magnetic field, frequency, and temperature have been calculated from simplified expressions for the spin-phonon transition probabilities of an $S = 3/2$ ion. The relaxation times for very low Cr^{3+} concentrations in $\text{K}_3\text{Co}(\text{CN})_6$, Al_2O_3 , and $\text{RbAl}(\text{SO}_4)_2 \cdot 12\text{H}_2\text{O}$ have been measured by the resonance-dispersion method at frequencies of 0.89 and 9.4 Gc/s, and at temperatures in the one-phonon relaxation region. A comparison of these as well as other published measurements with the calculations shows that the changes in relaxation time are usually predicted to better than a factor of two.

Calculations have shown that the resonance-dispersion analysis of experimental data, which is based on a two-level system, should yield single-valued relaxation times in the case of multi-level systems as well, and the results should be equal to those of pulse-saturation measurements where the return to equilibrium in the latter case can be characterized by a simple exponential.

ACKNOWLEDGEMENTS

The author feels in various ways indebted to several members of staff and students at the Eaton Electronics Laboratory, some of whom are no longer there: to Professor G.W. Farnell for his help and guidance throughout the course of this work; to Dr. J A. Carruthers without whose help and encouragement this research may have never been initiated; to Mr. C F. Weissfloch who kindly provided experimental data and helped with some of the measurements, and who contributed many hours of stimulating discussion; and to Dr. D. Fry for much helpful advice during the author's "freshman" period in computer programming.

Special thanks are due to my wife for giving up many precious hours to type this thesis.

This work was supported by grants to the Eaton Electronics Research Laboratory from the Defence Research Board and the National Research Council. The author is grateful to the Government of the Province of Quebec for a Bourse de Perfectionnement and to the Northern Electric Company for a fellowship held during the 1964-5 academic session.

TABLE OF CONTENTS.

I.	INTRODUCTION.	1
II.	THEORY OF SPIN-LATTICE RELAXATION.	
	1. The Interaction Hamiltonian.	7
	2. Spin-Phonon Transition Probabilities for the Direct Process.	10
III.	THE MEASUREMENT OF SPIN-LATTICE RELAXATION TIMES.	
	1. Relaxation Times in a $S=\frac{1}{2}$ Spin System.	15
	2. Pulse Saturation Measurements on a $S > \frac{1}{2}$ System.	17
	3. Steady-state Saturation Measurements on a $S > \frac{1}{2}$ System.	18
IV.	THE RESONANCE-DISPERSION TECHNIQUE.	
	1. Theory for a Two-level System.	
	a. Saturation theory.	19
	b. The dispersion equations.	22
	c. Experimental procedure.	23
	d. Cole-Cole dispersion diagram.	25
	e. Reduction of data.	27
	2. Extension of Method to Multi-level Systems.	28
V.	THE PARAMAGNETIC SALTS.	
	1. Cr^{3+} in Al_2O_3 .	32
	2. Cr^{3+} in $\text{K}_3\text{Co}(\text{CN})_6$.	33
	3. Cr^{3+} in $\text{RbAl}(\text{SO}_4)_2 \cdot 12\text{H}_2\text{O}$.	33
VI.	APPARATUS.	35

VII.	PROCEDURE.	
	1. Experimental.	38
	2. Calculations.	40
VIII.	RESULTS AND DISCUSSION.	
	1. Cr^{3+} in $\text{K}_3\text{Co}(\text{CN})_6$.	43
	2. Cr^{3+} in Al_2O_3 .	50
	3. Cr^{3+} in $\text{RbAl}(\text{SO}_4)_2 \cdot 12\text{H}_2\text{O}$.	61
	4. The Slopes in the Logarithmic Plots of T_1 versus $1/Z$.	64
	5. Calculations for Steady-State Saturation Conditions.	67
IX.	CONCLUSIONS.	68
X.	BIBLIOGRAPHY.	72
APPENDIX I	- Calculation of Relaxation Times.	75
APPENDIX II	- "Measurement of Spin-Lattice Relaxation at 890 Mc/s by a Resonance-Dispersion Technique", by J.A. Carruthers and N.C. Rumin (Reprint).	78

I. INTRODUCTION

When the thermal-equilibrium energy distribution of a group of paramagnetic ions, whose paramagnetism is due to a net magnetic dipole moment associated with their spins, is in some way disturbed, the subsequent return to equilibrium is said to take place through spin-lattice relaxation if it occurs as the result of the exchange of energy-conserving quanta between the spins and the thermal spectrum of the host lattice.

From the early work of Waller, Casimir and DuPré, Kronig, and Van Vleck*, and a later re-examination of Van Vleck's work by Mattuck and Strandberg (1960), the spin-lattice interaction of paramagnetic ions in crystals is understood to occur through the thermal modulation of the crystalline electric field. The theory predicts that at very low temperatures, T , the spin-lattice transition probability, w_{ij} , between spin states i and j will be determined by a direct, one-phonon process with w_{ij} varying as T , while at higher temperatures a two-phonon, Raman mechanism will dominate with w_{ij} varying as T^7 or T^9 .

In the case of a two-level system the return to equilibrium of the population of levels 1 and 2 is characterized by a spin-lattice relaxation time T_1 where $T_1 = 1/2w_{12}$. No such simple relationship exists in the case of multi-level systems but an effective spin-lattice relaxation time T_R is still used to describe the return to equilibrium of the population of a pair of levels, even though this generally involves all the

*Woonton (1961) furnishes an excellent bibliography related to theoretical and experimental work on spin-lattice relaxation.

other spin levels as well.

Much of the early theoretical and experimental work was centred on the ions of the 3d iron group. The measured values of T_R often did not agree well with the theory, and explanations for some of the inconsistencies were proposed by Bloembergen et al (1959), who considered the role played by cross-relaxation, and by Bloembergen and Pershan (1961), Van Vleck (1961), and Gill and Elliot (1961), who extended the concept of cross-relaxation to excited states.

Several effects predicted by the theory of spin-lattice relaxation have been verified experimentally. Thus Pace et al (1960) and Feng and Bloembergen (1963) have verified the inverse temperature dependence for the $S=3/2$ Cr^{3+} ion in Al_2O_3 at low temperatures, while Paxman (1960), Rannestad and Wagner (1963), and Scott and Jeffries (1962) have observed the changeover with temperature from the single phonon process to the highly temperature dependent Raman mechanism, for $S=1/2$ ions of both the iron and rare earth groups. Davids and Wagner (1964) were able to verify that for an $S=1/2$ ion such as Fe^{3+} in $K_3Co(CN)_6$ the spin-lattice relaxation time at temperatures where the one-phonon process dominates, varies with the steady magnetic field H as H^{-4} .

Experimental data on the field and frequency dependence of the spin-lattice relaxation time in multi-level spin systems are rather scarce if one excludes measurements made by the nonresonant method of Gorter and his group, which are difficult to interpret in terms of the theories considered here. Generally

the measurements do not show any strong dependence of T_R on either H or the resonant frequency ν . An experimental investigation of the dependence of relaxation time on these two parameters in potassium chromicyanide was started here by this author (Rumin 1961), and the measurements were repeated by Carruthers and Rumin (1965) using the resonance-dispersion method. Because those measurements did not show the strong ν^{-2} dependence reported for this salt (Van Vleck 1961) it was decided to re-examine the implications in the results of Van Vleck's theory of spin-phonon interaction when applied to multi-level systems, particularly in the light of the more general treatment by Mattuck and Strandberg (1960). Because the exact calculation of spin-phonon transition probabilities is extremely difficult it was decided to use, at least as a first attempt, the order of magnitude expressions obtained by Mattuck and Strandberg (1960). Calculations were under way, yielding very promising results, when Donoho (1964) published his work on ruby in which he carried out detailed calculations of relaxation times from published experimental data on the elastic properties of ruby. His work provided a certain amount of justification for the use of Mattuck and Strandberg's approximate equations, at least in the case of ruby. It also confirmed what our calculations for potassium chromicyanide had already shown, namely that the frequency dependence of the one-phonon, spin-lattice relaxation time for salts such as ruby or potassium chromicyanide, where there is zero-field splitting of the ground state, is not as strong as is implied by the ν^2

term which appears in the approximate expression for the spin-phonon transition probability. From measurements on ruby and some rough calculations Feng and Bloembergen (1963) concluded that the relaxation time is essentially independent of H below 4000 gauss and thereafter decreases approximately linearly with H to 15000 gauss. Just as Donoho, they suggested that this behavior may be explained by the zero-field splitting which was not taken into account in Van Vleck's calculations.

As it was pointed out above, the calculations of spin-phonon transition probabilities is extremely difficult and cannot, in general, be carried out without an appreciable number of approximations. Furthermore, experimental data which would facilitate this calculation, such as the elastic strain data that were used by Donoho (1964), have been obtained for only one or two host lattices, and may not be forthcoming for the remaining large number of crystals for some time. Consequently, a primary objective of the present work was to investigate the accuracy with which the variations of the one-phonon, spin-lattice relaxation time with magnitude and direction of the steady magnetic field, frequency, and temperature could be predicted for a given ion-host lattice combination from a highly simplified theory. Using two spectrometers, one operating at 0.89 Gc/s and the other at 9.4 Gc/s, relaxation times were measured for very low concentrations of Cr^{3+} in potassium cobalticyanide, rubidium alum, and aluminum oxide. These results as well as other published data indicate that the changes in relaxation

time can be predicted usually to well within a factor of two, from calculations in which only the quadratic spin operator and temperature and frequency dependent terms are retained in the calculation of the spin-lattice transition probabilities.

Because Donoho (1964) provides detailed calculations of the angular dependence of spin-lattice relaxation times in ruby at 9.3 Gc/s, a second objective of this work was to verify these experimentally. For reasons discussed in a later chapter, one can only conclude from the measurements that Donoho's calculations, as well as those reported here, predict the general behavior of the changes in the relaxation time with the magnitude and orientation of the dc magnetic field.

Relaxation times have usually been measured by either the pulse saturation technique (Bowers and Mims 1958) or the steady-state saturation method (Bloembergen et al 1948). More recently Carruthers and Rumin (1965) proposed the resonance-dispersion method. Because the technique employs an analysis based on a two-level system but was used by them and in this work for measurements on multi-level systems, it was deemed important to establish the validity of this approach. Calculations indicate that, subject to certain restrictions which experimental data indicates are usually satisfied in the case of dilute paramagnetic crystals, the three methods should yield the same results. These conclusions were confirmed by measurements on potassium chromicyanide. There is thus appreciable justification for the use of the resonance-dispersion method which does not suffer from many of the inaccuracies associated with the

steady-state saturation technique, and which is more suited to measurements on lines having intensities that, in general, preclude the use of the more straightforward pulse saturation method.

The concentration dependence of relaxation times, which is not predicted in the theory of spin-lattice relaxation, has been observed by Gill (1962), Mims and McGee (1960), Pace et al (1960), to name just a few. Carruthers and Rumin (1965) also observed a concentration dependence in their resonance-dispersion measurements on potassium chromicyanide at 0.89 Gc/s and 4.2° Kelvin, which manifested itself in a manner that made the determination of the true spin-lattice relaxation time difficult. Their suggestion that this effect would become negligible at sufficiently low concentration, making the experimental data easier to interpret, has been confirmed in this work, and it has also been shown that at 0.89 Gc/s the single-phonon, spin-lattice relaxation mechanism is still not dominant at 4.2°K in potassium chromicyanide at the field of 340 gauss where most of their measurements were made.

II. THEORY OF SPIN-LATTICE RELAXATION.

In the study of paramagnetic relaxation phenomena, the interaction between the paramagnetic spins and the phonon field of the host lattice plays an important role. As noted in the introduction, explanations of the process of energy transfer between the spins and the lattice were proposed by Kronig (1939) and Van Vleck (1940), while Mattuck and Strandberg (1960) presented a more general treatment of the problem. The energy transfer is understood to take place principally via two mechanisms, a direct process in which a spin absorbs (or emits) a phonon of energy equal to the spin transition, and a Raman process in which two phonons whose energy difference is equal to the spin transition participate. An outline of the theory of spin-lattice relaxation is presented on the following pages, the treatment following closely that of Mattuck and Strandberg.

II.1. The Interaction Hamiltonian.

The theory of spin-lattice interaction is developed on the basis of a model in which the paramagnetic ion is acted on by an electric field produced by the surrounding ligands. Since the ligands are part of the crystal lattice they vibrate, and this results in a modulation of the electric field, which perturbs the orbital motion of the paramagnetic electrons, and in turn induces spin transitions by means of spin-orbit interaction.

If one assumes that the crystal is sufficiently dilute that the effects of spin-spin coupling are negligible, then

one can describe the state of a paramagnetic ion by a Hamiltonian of the form

$$(1) \mathcal{H} = \mathcal{H}_L + \mathcal{H}_0 + V + 2\beta \vec{S} \cdot \vec{H} + \lambda \vec{L} \cdot \vec{S} + \beta \vec{L} \cdot \vec{H}$$

where \mathcal{H}_L is the lattice energy, \mathcal{H}_0 is the energy of the free ion, V is the crystalline field potential at the ion, β is the Bohr magneton, λ is the spin-orbit coupling constant, \vec{H} is the external dc magnetic field, and \vec{S} and \vec{L} are the spin and orbital angular momenta of the ion.

Since it is only the modulation on the crystalline electric field which induces spin transitions, a plausible approach to the problem is to express V in terms of a static and a time-dependent part, and then to treat the latter as a perturbation on the total Hamiltonian \mathcal{H} . This is done by expanding V in a power series in the normal displacements Q_f of the paramagnetic ion's nearest neighbors, which are in turn expanded in normal lattice modes. As a result V can be put in the form

$$(2) V = V_0 + V_I$$

where V_0 is the static portion of V , and V_I is the modulation of V_0 . The total Hamiltonian can now be written in the form

$$(3) \mathcal{H} = \mathcal{H}_L + \mathcal{H}_S + \mathcal{H}_I$$

where $\mathcal{H}_I = V_I$, and

$$\mathcal{H}_S = \mathcal{H}_0 + V_0 + 2\beta \vec{S} \cdot \vec{H} + \lambda \vec{L} \cdot \vec{S} + \beta \vec{L} \cdot \vec{H}.$$

The term \mathcal{H}_S involves only paramagnetic electron coordinates and, when diagonalized to second order, gives rise

to the spin Hamiltonian which describes the energy levels that result from the splitting of the ground state by the laboratory dc field H. In spin-lattice relaxation experiments one is interested in the phonon-induced transition probabilities between pairs of these spin levels. If, following the approach outlined above, one considers \mathcal{H}_I to be a perturbation inducing energy-conserving exchanges of quanta between \mathcal{H}_S and \mathcal{H}_L , the transition probabilities are calculated by diagonalizing \mathcal{H}_S , evaluating its eigenvalues E_k and eigenvectors ψ_k , and computing the appropriate matrix elements of \mathcal{H}_I between simultaneous eigenstates of \mathcal{H}_S and \mathcal{H}_L .

The proposed computation is quite difficult, in part due to the fact that the ψ_k are complicated mixtures of both orbital and spin states, since they contain the effect of the excited states on the ground level. Mattuck and Stranberg show that the evaluation of matrix elements of \mathcal{H}_I between the ψ_k 's is equivalent to calculating, for the single-phonon process, matrix elements of a spin-phonon interaction Hamiltonian \mathcal{H}_D between the relatively simple spin functions ϕ_k of the spin Hamiltonian which is produced when \mathcal{H}_S is diagonalized to second order. Their equation (44) for \mathcal{H}_D has the form:

$$(4) \quad \mathcal{H}_D = \sum_{p,f,i,j} A^{fp} (a_p^\dagger + a_p) \left\{ \text{terms } O(\lambda\beta HS_i) + \lambda^2 \mathcal{L}_{ij}^f S_i S_j \right\},$$

where a_p^\dagger and a_p are the creation and annihilation operators corresponding to the normal lattice mode-branch p, $A^{fp} (a_p^\dagger + a_p)$ is the normal displacement corresponding to nearest neighbor mode f and lattice mode-branch p, S_i and S_j are spin operators

(i and j being x,y, or z) and λ_{ij}^f is a tensor which contains the effect of the excited states.

The problem of calculating the spin-phonon transition probabilities is thus reduced to one of calculating matrix elements of \mathcal{H}_D involving the comparatively simple wave functions ϕ_k of the spin Hamiltonian.

The expression corresponding to equation (4) for the Raman process is much more complex and will not be given since it is of little interest insofar as the work reported here is concerned.

II.2 Spin-Phonon Transition Probabilities for the Direct Process.

It is in the evaluation of \mathcal{H}_D , more specifically, of A^{fp} and λ_{ij}^f , that severe difficulties are encountered in the calculation of spin-phonon transition probabilities. Although it is possible to express the spin-phonon interaction Hamiltonian in terms of the normal modes of an isolated cluster of nearest neighbor atoms, there remains the very complex problem of relating these to the physical constants of the host lattice of which the cluster is a part. Investigators have consequently resorted to averages over the modes which, in the end, remove many of the physical properties of the host lattice from the calculation.

Using the simple model of a paramagnetic ion at the origin with two nearest neighbors of charge e lying at $x = \pm R$, Mattuck and Strandberg obtain the following crude formula for order-of-magnitude calculations of the interaction

Hamiltonian \mathcal{H}_D :

$$(5) \quad \mathcal{H}_D \sim \sum_i K \nu_p^{\frac{1}{2}} (a_p^\dagger + a_p) [\lambda^2 S_A + \text{terms } O(\lambda \beta H S_i)],$$

where S_A is the spin anticommutator ($S_x S_y + S_y S_x + S_x S_z + S_z S_x + S_y S_z + S_z S_y$), and some of the terms in their expression for \mathcal{H}_D which are constants for a given ion and host lattice have been grouped into the constant K . Equation (5) assumes an average over phonons of all propagation directions, polarizations and phases.

Since the particular model considered here is used primarily to estimate the size of the Λ_{ij}^f , with the resulting terms being all grouped into the constant K , it is assumed in what follows that equation (5) applies in form to a more physical model. In fact, a comparison of equation (5) with the more exact equation (4) reveals that the approximation which is implicit in obtaining (5), insofar as the Λ_{ij}^f terms are concerned, is

$$\sum_f \Lambda_{xx}^f = \sum_f \Lambda_{yy}^f \quad \text{and} \quad \sum_f \Lambda_{xy}^f = \sum_f \Lambda_{xz}^f = \sum_f \Lambda_{yz}^f.$$

The magnitudes of the Λ_{ij}^f were estimated for ruby from data presented by Donoho (1964) and the results indicate that, at least for this salt, the above approximation is not an unreasonable one.

For the direct process, the spin-phonon transition probability between states k and k' is:

$$(6) \quad w_{kk'} = \frac{1}{\pi^2} |\langle p'k' | \mathcal{H}_D | pk \rangle|^2 \rho(\nu_r)$$

where ν_r is the resonance frequency between the two levels and $\rho(\nu_r)$ is the density of states in the phonon field. If it is assumed that the lattice is dispersionless and isotropic, then the phonon density can be described by the Debye equation

$$(7) \quad \rho(\nu) = \frac{12 \pi \nu^2}{\mathcal{V}^3}$$

where \mathcal{V} is the phonon velocity.

The operators a_p and a_p^\dagger in equation (6) have the properties :

$$(8) \quad a_p^\dagger |n_p\rangle = (n_p + 1)^{\frac{1}{2}} |n_p + 1\rangle$$

$$a_p |n_p\rangle = (n_p)^{\frac{1}{2}} |n_p - 1\rangle$$

Upon substituting equations (5) and (7) into (6) and making use of (8) and the fact that the average number of phonons in mode p , when the lattice is in thermal equilibrium at a temperature T , is given by

$$(9) \quad \bar{n}_p = [\exp(h\nu_p/kT) - 1]^{-1},$$

the transition probability for an emission process between a spin state k and a lower one k' is

$$(10) \quad w_{kk'} = \sum_i K' \frac{\nu_r^3 \exp(h\nu_r/kT)}{\exp(h\nu_r/kT) - 1} |\langle k | \lambda^2 S_A + \text{terms } O(\lambda\beta HS_i) | k' \rangle|^2$$

$$\text{where } K' = 12 \pi K^2 / \hbar^2 \mathcal{V}^3.$$

The spin-orbit coupling constant for many paramagnetic ions, including Cr^{3+} , is of the order of 100 cm^{-1} . Hence, for fields of a few thousand oersteds $\lambda\beta H$ is approximately two orders of magnitude smaller than λ^2 and, therefore, the $\lambda\beta HS_i$ terms may be dropped when S_A is of the order of unity. They will be dropped in all cases, since when the contribution of S_A is

small the addition of these terms will not markedly affect the magnitude of $w_{kk'}$, which will also be small and will, therefore, not contribute significantly to the spin-lattice relaxation process involving the $2S + 1$ levels of an $S > \frac{1}{2}$ ion. Hence equation (10) simplified to:-

$$(11) \quad w_{kk'} = \frac{K'' \nu_r^3 \exp(h \nu_r / kT)}{\exp(h \nu_r / kT) - 1} |\langle k | S_A | k' \rangle|^2$$

$$\text{where } K'' = K' \lambda^4.$$

It should be noted that equation (11) is not valid for $S = \frac{1}{2}$ ions since the spin anticommutator S_A does not connect $-\frac{1}{2}$ and $\frac{1}{2}$ states, and the terms linear in S_i can not in fact be dropped.

Although in the calculations reported here the $w_{kk'}$ were always calculated from equation (11), it is instructive to consider the form of this expression under the high temperature approximation $h \nu_r \ll kT$. In this case the terms multiplying the matrix elements simplify to $K'' T \nu_r^2$. However, because the matrix elements are evaluated between spin states which, in general, are mixed, the amount of mixing being dependent on the magnitude and orientation of the dc magnetic field H , the $w_{kk'}$ will depend on these two parameters as well and, consequently, the frequency dependence should, in general, be different from that implied by the ν_r^2 term. Because the high temperature approximation seems to hold quite well for a major portion of the experimental data considered in this work, it is important to note that, in using equation (11) under conditions where the approximation is valid, one assumes that the

relative magnitudes of spin-phonon transition probabilities for the direct process are determined by the product of the temperature, the square of the resonant frequency, and the square of the spin anticommutator matrix elements.

III. THE MEASUREMENT OF SPIN-LATTICE RELAXATION TIMES.

A large portion of the study of paramagnetic relaxation is concentrated on the measurement of spin-lattice relaxation times, and the subsequent comparison with calculations based on theories such as the one outlined in Section II. Even under conditions where the single-phonon process is the dominant mechanism in determining the rate of energy transfer between the spins and the bath in which the crystal is immersed, relating measurements to theory is often complicated by the fact that for multi-level spin systems all the levels, in general, participate in the spin-lattice relaxation process even though resonant excitation is applied to only a pair of levels. This problem will be considered in terms of two established techniques of measuring relaxation times. A discussion of the difficulties which arise in the case of the resonance-dispersion technique, which was used to obtain the measurements reported here, is left to a separate chapter.

III.1. Relaxation Times in a $S=\frac{1}{2}$ Spin System.

In the absence of resonant radiation, the differential equations governing the time dependence of the populations of the two levels into which the ground state is split by a laboratory dc field H are

$$(12) \quad n_1 = -w_{12}n_1 + w_{21}n_2$$

$$n_2 = w_{12}n_1 - w_{21}n_2$$

In the high temperature approximation ($\hbar\omega \ll kT$) these can be transformed into a single equation (Andrew 1956)

$$(13) \quad \dot{n} = 2w(n_0 - n)$$

where n is the excess number of spins in the lower state, n_0 is the thermal equilibrium value of n , and w is the mean of the two spin-phonon transition probabilities w_{12} and w_{21} . The solution of (13) is

$$(14) \quad n/n_0 = 1 - (1 - n_a/n_0)\exp(-2wt)$$

where n_a is the initial value of n . Thus the approach of the spin system and the lattice to thermal equilibrium can be characterized by a spin lattice relaxation time T_1 where $T_1 \cong 1/2w$.

In the presence of resonant radiation, equation (13) becomes

$$(15) \quad \dot{n} = 2w(n_0 - n) - 2nP$$

where P is the radiation-induced transition probability. Under steady state conditions $\dot{n} = 0$ and the solution of (15) for the steady state population difference n_s is

$$(16) \quad n_s/n_0 = (1 + P/w)^{-1} \cong Z$$

where Z is the saturation factor.

Equations (14) and (16) are the basis of two techniques for measuring T_1 and, hence, w . In the steady-state saturation technique (Bloembergen et al 1948) one essentially measures Z as a function of the intensity of the resonant rf field. P depends on the intensity of the rf field, the line-shape factor $g(\nu)$, and the wave functions ϕ_k associated with the two

levels, and can, in principle, be calculated. Hence w can be evaluated from (16).

In the pulse saturation technique (Bowers and Mims 1959), rf excitation is applied in the form of a pulse having an amplitude and duration sufficient to drive the spin system into steady-state saturation, i.e. cause $n_s \leftrightarrow 0$. The return to equilibrium of the spin system after the end of the pulse is evidently given by equation (14) with $n_a = 0$. A small monitor signal is used to observe the behavior of n/n_0 as a function of time and hence w is obtained directly from a semilogarithmic plot of the monitor signal level versus time.

Thus for a $S = \frac{1}{2}$ system one can measure the spin-phonon transition probability between the pair of levels to which resonant excitation is applied.

III.2. Pulse Saturation Measurements on a $S > \frac{1}{2}$ System.

For a spin system with $S > \frac{1}{2}$ there are $2S + 1$ levels. The rate equations which describe the dynamic behavior of the spin system are (Lloyd and Pake 1954):

$$(17) \quad \dot{n}_i = \sum_j (w_{ji} n_j - w_{ij} n_i)$$

where n_i is the population of the i -th level. When a pair of levels, say 1 and 2, are subjected to resonant excitation, w_{12} and w_{21} in equations (17) must be replaced by $w_{12} + P$ and $w_{21} + P$, respectively. The solution for the return to equilibrium of the populations of levels 1 and 2 after a pulse of rf power sufficient to saturate the pair of levels, is given, in

the case of four levels, by (Andrew and Tunstall, 1961)

$$(18) \quad (n_1 - n_2) / (n_{10} - n_{20}) = 1 - A_1 \exp(-t/T_1) - A_2 \exp(-t/T_2) - A_3 \exp(-t/T_3)$$

where each of the time constants T_1 , T_2 and T_3 is a complicated combination of the w_{ij} 's. More generally, the number of time-dependent terms is one less than the number of levels. Thus in the case of a multi-level system a pulse saturation measurement will not, in general, yield the spin-phonon transition probability between a given pair of levels, even in cases where the relationship between the terms in equation (18) is such that the equation can be closely approximated by a simple exponential.

III.3. Steady-state Saturation Measurements on a $S > \frac{1}{2}$ System.

Under conditions of steady-state rf excitation of transitions between levels k and l , the saturation factor $Z = (n_k - n_l) / (n_{k0} - n_{l0})$ is obtained by solving equations (17) with all the $\dot{n}_i = 0$ and w_{1k} and w_{k1} replaced by $w_{1k} + P$ and $w_{k1} + P$, respectively. The solution is (Lloyd and Pake, 1954)

$$(19) \quad Z = (n_k - n_l) / (n_{k0} - n_{l0}) = (1 + P/W)^{-1}$$

where W is a complicated expression involving all the w_{ij} 's. Equations (19) and (16) are identical except for the fact that W in equation (19) is an effective relaxation probability that is not related in any simple way to w_{k1} .

IV. THE RESONANCE DISPERSION TECHNIQUE.

The resonance-dispersion technique for measuring relaxation times has been described by Carruthers and Rumin (1965)* and is presented here in a condensed form. It is similar to both the steady-state saturation method and the audio-frequency relaxation approach (Waller 1932, Gorter 1947). The dispersion of the incremental susceptibility at audio modulation frequencies is observed at various levels of saturation, produced by resonance absorption at the rf frequency. The dispersion observed can be related to the spin-lattice relaxation time by extending saturation theory to include the effect of fluctuating spin populations during the modulation cycle.

Because the theory for this technique has been worked out in detail only for a two-level system, the effect of using this method on multi-level systems will be discussed.

IV.1. Theory for a Two-level System.

a. Saturation theory.

Experimental measurements in both the steady-state saturation and the resonance-dispersion techniques are based on determining the power absorbed in the paramagnetic sample as a function of incident power. The power absorbed per unit volume of the sample is given by

$$(20) \quad \mathcal{P} = (n_2 - n_1) \nu h P$$

*A copy of the paper is included at the end of the thesis as Appendix II.

The power can also be expressed in terms of the imaginary component of the complex susceptibility, χ'' , and the rf field strength, H_1 (Andrew 1956):

$$(21) \quad P = 4\pi\nu\chi''H_1^2$$

The radiation induced transition probability can be written as

$$(22) \quad P = JH_1^2g(\nu)$$

where J is a constant for a given dc magnetic field \vec{H} .

Combining equations (20), (21), and (22), and making use of the definition of the saturation factor Z , yields the following result:

$$(23) \quad \chi'' = KZg(\nu)$$

$$\text{where } K = [(n_{20} - n_{10})hJ] / 4\pi$$

For measurements of the transition probability w by the steady-state saturation technique only relative values of χ'' are important. It is seen from equation (21) that χ'' is proportional to the ratio of the power absorbed to the power incident, and the change in this ratio, as saturation occurs, is all that needs to be measured to determine Z . The transition probability w is then calculated using equations (22) and (19).

In practice it is customary to use magnetic field modulation and synchronous detection to obtain a better signal-to-noise ratio. The magnetic field H is modulated at an audio frequency ω , while H is swept slowly through the line. The modulation amplitude is kept small compared to the resonance linewidth and the curve traced out on the recorder is proportional to the slope of the χ'' versus H plot (Rumin 1961).

One is therefore interested in the differential of χ'' which can be obtained from equation (23). Since it is H that is varied and not ν , the line shape factor $g(\nu)$ should be replaced by $g(H)$ where

$$\int_0^{\infty} g(H) dH = 1$$

The result is

$$(24) \quad d\chi'' = K[Zdg(H) + g(H)dZ].$$

It is now interesting to consider the effect of the modulation frequency ω on $d\chi''$. When ω is small compared to the spin-phonon transition probability, the spin population readjust quickly enough during the modulation cycle for stationary conditions to be assumed to apply at all times. Hence from equations (24), (19), and (22)

$$(25a) \quad d\chi'' = KZ^2 dg(H)$$

at very low modulation frequencies.

When ω is very large compared to w_{ij} the spin population can be assumed to be constant during the modulation cycle. Hence $dZ = 0$ and one obtains

$$(25b) \quad d\chi'' = KZdg(H)$$

Equations (25a) and (25b) show that if H is set at some arbitrary point of a partially saturated line and the modulation frequency is slowly varied, a form of dispersion should be observed with the signal at a very high frequency greater than that at a very low frequency by the factor $1/Z$. This dispersion results because the spin-lattice relaxation probability is

comparable to the modulation rate over a particular range of modulation frequencies. In the next section the dispersion region is examined more fully in order to show how this effect can be used to advantage in measurements of spin-lattice relaxation time.

b. The dispersion equations.

Equation (15) describes the behavior of the excess number of spins in the lower state when resonant rf power is applied. When sinusoidal modulation is applied to the magnetic field the line-shape factor $g(H)$ is caused to fluctuate, and if the modulation amplitude is small the $g(H)$ term is sine-wave modulated. Now P is proportional to $g(H)$ and hence P can be written as

$$(26) \quad P = \bar{P} [1 + a \exp(j\omega t)]$$

where a is small compared to unity.

Assume a solution for n of the same form as for P ,

$$(27) \quad n = \bar{n} [1 + b \exp(j\omega t)] .$$

Substitution of equations (26) and (27) into (15) yields an expression which can be separated into two parts, one involving the mean values, the other containing the time-varying terms:

$$(28a) \quad \bar{n}/n_0 = (1 + \bar{P}/w)^{-1}$$

$$(28b) \quad \bar{n}b(2w + j\omega) + 2\bar{n}\bar{P}(a + b) = 0$$

Here a small, second-harmonic term which would be rejected by the synchronous detector has been dropped.

Equation (28a) is identical to equation (16) defining the saturation factor Z . Equation (28b) involves the amplitudes

of the alternating components and hence must contain information on the dispersion. But to use this equation for experimental determinations of w it is necessary to interpret the equation in terms of a particular experimental procedure. For future reference equation (28b) is rewritten using the definition of Z and substituting T_1 for $1/2w$:

$$(29) \quad (a + b)/a = (Z + j\omega ZT_1)/(1 + j\omega ZT_1),$$

c. Experimental procedure.

The spectrometer, described more fully in Section VI, is of the bridge type with a heterodyne receiver. The audio-frequency signal from the linear detector of the I.F. system is fed to an amplifier and phase-sensitive detector.

Consider that the dc magnetic field is set at a particular value somewhere near the center of the absorption line and that the bridge is adjusted so as to be sensitive to the imaginary component of the incremental susceptibility, $d\chi''$. The magnetic field is modulated over an amplitude range that is small compared to the linewidth.

The rf power is first set to a very low level so that saturation effects are negligible. The phase-sensitive detector and recorder are adjusted to give a good deflection, it being understood that any phase shift in the modulation coils and in the audio system can be balanced out. Several measurements can now be made at different power levels, and at other modulation frequencies, to determine the effect of power level

and modulation frequency on the phase and magnitude of the output signal.

In a spectrometer employing a heterodyne receiver the amplitude of the signal is proportional to the incremental power absorbed in the sample. Making use of equations (20), (26) and (27) we obtain for the incremental power $d\mathcal{P}$

$$(30) \quad d\mathcal{P} = h\nu \bar{n}\bar{P}(a + b)e^{j\omega t}$$

where the second-harmonic term has been neglected.

The rf field H_1 is proportional to the square root of the input power. Therefore, according to the procedure outlined above, the relative signal from the phase-sensitive detector is proportional to $d\mathcal{P}/H_1^2$ which, from equations (30) and (22), is given by

$$(31) \quad d\mathcal{P}/H_1^2 = [h\nu n_o J\bar{g}(H)] Z(a + b)e^{j\omega t}$$

where Zn_o has been written in the place of \bar{n} , and $\bar{g}(H)$ is the average value of $g(H)$ over the modulation cycle.

When the input power level is low enough for saturation effects to be negligible, we have that $Z \rightarrow 1$ and n is effectively constant. Hence $b \rightarrow 0$ as $Z \rightarrow 1$, and the term $(a + b) \rightarrow a$. This unsaturated condition corresponds to maximum relative signal strength.

From equation (31) the effect of saturation on the relative signal strength is determined by the product $Z(a + b)$. If the ratio of the relative signal strength when the system is partially saturated to that when $Z = 1$ is denoted by A , then

$$(32) \quad A = [Z(a + b)] / a$$

Making use of equation (29) and letting $A = A' + jA''$ and $\tan \Theta = A''/A'$, we obtain

$$(33) \quad A' = Z(Z + \omega^2 Z^2 T_1^2) / (1 + \omega^2 Z^2 T_1^2)$$

$$(34) \quad \tan \Theta = \omega Z T_1 (1 - Z) / (Z + \omega^2 Z^2 T_1^2) .$$

A' , and $\tan \Theta$ are measurable quantities. Using equations (33) and (34), and knowing ω , it is possible to deduce values of both Z and T_1 . But since the equations are not linear in T_1 there is possible ambiguity in the reduction of data. In this respect it is instructive to interpret the dispersion in terms of a Cole-Cole diagram (Cole and Cole 1941).

d. Cole-Cole dispersion diagram.

With the substitution of τ for ZT_1 , the attenuation A can be written as:

$$(35) \quad A = Z(Z + j\omega\tau) / (1 + j\omega\tau)$$

By rearrangement,

$$(36) \quad (Z - Z^2) = (Z - A) + j\omega\tau(Z - A)$$

The amplitude A is plotted in the complex plane in terms of its real and imaginary components A' and A'' in Figure 1. If only ω is allowed to vary, equation (36) shows that the locus of A is a semicircle which crosses the A' axis at $A' = Z$ and $A' = Z^2$, when $\omega = \infty$ and $\omega = 0$, respectively.

For a particular value of ω the locus of A is constrained to lie only within the region represented by the family of semicircles corresponding to different values of Z . The path followed by A as Z is varied depends primarily on

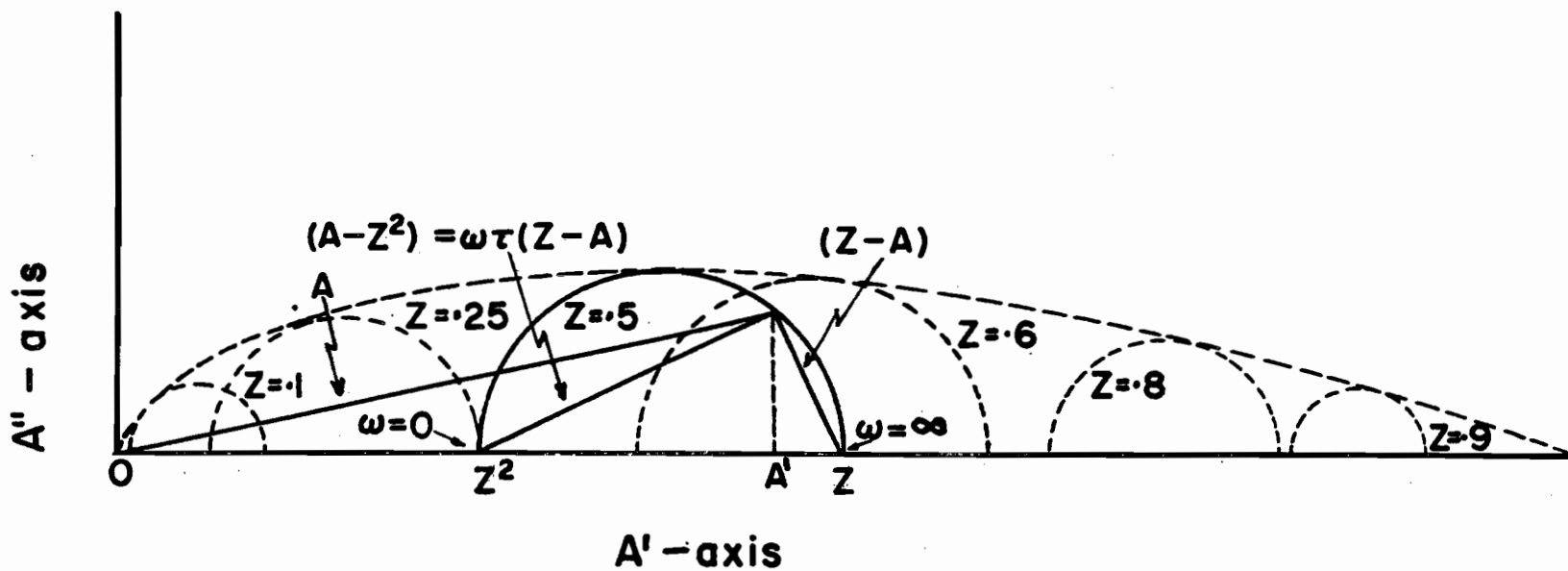


Figure 1. Cole-Cole diagram for relative signal amplitude when saturation is present.

the value of ωT_1 , and if $\omega T_1 \gg 1$ the path is along the A' axis until very small values of Z are obtained. The modulation frequencies are therefore chosen so that measurable phase shifts occur when Z is somewhere in the range 0.5-0.01.

e. Reduction of data.

From Figure 1, because $(Z - A)$ and $(A - Z^2)$ are perpendicular, it follows that

$$(37) \quad (A'')^2 = (Z - A)(A' - Z^2)$$

which, upon substituting $A' \tan \Theta$ for A'' , gives

$$(38) \quad Z^3 - A'Z^2 - A'Z + (A')^2(1 + \tan^2 \Theta) = 0$$

Since equation (38) is cubic in Z , there are three roots. Of these one is negative and can be neglected. The presence of two allowable solutions for Z follows from the observation that a measured value of A can correspond to two of the Cole-Cole semicircles. If Θ is close to the maximum angle permitted for A , the two solutions for S are very nearly equal and it is difficult to decide which is the correct one. Hence, for each modulation frequency it is advisable to keep the power level below that for which this condition arises. A useful criterion is that $Z > 1/\omega T_1$. If this precaution is observed, the correct solution for Z is the smallest of the two allowable roots of equation (38).

The method of successive approximations is a simple means for finding the roots of equation (38). The equation may be rewritten in a form which lends itself to this approach:

$$(39) \quad Z = A' \left[1 + \frac{A'}{A' - Z^2} \tan^2 \Theta \right]$$

and which yields the lower of the two allowable roots. The approximate relation corresponding to equation (39) is:

$$(40) \quad Z \doteq A' \left[1 + \frac{\tan^2 \Theta}{1 - A'} \right]$$

and can be used to obtain the first approximation to the correct value of Z.

In the Cole-Cole diagram in Figure 1 $(A - Z^2) = \omega \tau (Z - A)$
Hence, from similar triangles,

$$\frac{\omega \tau (Z - A)}{(Z - A)} = \frac{(A' - Z^2)}{A''}$$

Putting $A'' = A' \tan \Theta$, and $\tau = Z T_1$, we have

$$(41) \quad T_1 = \frac{A' - Z^2}{A' Z \omega \tan \Theta}$$

Thus if the precaution $Z > 1/\omega T_1$ is observed, the correct value of T_1 and Z is obtained from equations (40), (39) and (41).

IV.2. Extension of Method to Multi-level Systems.

Because of the added complexity of considering more than two levels it has not been possible to extend the theory for the resonance-dispersion technique to multi-level systems. However, because pulse saturation measurements carried out at low temperatures on dilute crystals often yield essentially single time-constant decays, it is tempting to use the

resonance-dispersion theory as it stands on such crystals. This was in fact done by Carruthers and Rumin (1965) who noted that the X-band results of Castle et al (1960) show that it is often a good approximation to assume that a single-valued relaxation time occurs for the four-level Cr^{3+} ion in dilute crystals of $\text{K}_3\text{Co}(\text{CN})_6$. It is instructive to investigate the validity of such an approach even though the complexity of the problem forces one to numerical solutions.

Using the four-level system as an example, we obtain from equation (17) four equations in terms of the populations of the four levels. Taking the radiation induced transition probability P to be, as before, of the form

$$(26) \quad P = \bar{P} [1 + a \exp(j\omega t)]$$

we assume solutions for the four populations of the form:

$$(42) \quad n_i = \bar{n}_i [1 + b_i \exp(j\omega t)]$$

where $b_i = b_i' + j b_i''$, etc.

Let us assume that P acts between levels 2 and 3. Substituting equations (42) and (26) into equations (17) specialized to the four-level case, and replacing w_{23} and w_{32} by $w_{23} + P$ and $w_{32} + P$, respectively, we obtain four equations each of which, just as in the two-level case, can be separated into two parts. The four equations involving mean values are identical to the steady-state saturation equations for which the solution is given in equation (19):

$$(43) \quad (\bar{n}_2 - \bar{n}_3) / (n_{20} - n_{30}) = (1 + \bar{P}/W)^{-1}$$

The four equations containing the time-varying terms can be further separated into real and imaginary parts which gives eight equations in the eight unknown coefficients b_1' , b_1'' , b_2' , b_2'' , etc. These can, in principle, be solved.

Making use of equations (20), (26), (42b), and (42c) the power absorbed in the sample is

$$(44) \quad \mathcal{P} = h\nu\bar{P} \left\{ 1+a \exp(j\omega t) \right\} \left[\bar{n}_2 \left\{ 1+b_2 \exp(j\omega t) \right\} - \bar{n}_3 \left\{ 1+b_3 \exp(j\omega t) \right\} \right]$$

Hence the incremental power $d\mathcal{P}$ is, ignoring second-harmonic terms,

$$(45) \quad d\mathcal{P} = h\nu\bar{P} \left\{ \bar{n}_2(a+b_2) - \bar{n}_3(a+b_3) \right\} \exp(j\omega t)$$

Equation (45) can be manipulated in a manner similar to that used on equation (30) to yield the attenuation A:

$$(46) \quad A = \frac{\bar{n}_2(a+b_2) - \bar{n}_3(a+b_3)}{(n_{20} - n_{30})a}$$

Separating into real and imaginary parts, and letting $\tan\Theta = A''/A'$, we obtain

$$(47a) \quad A' = \frac{\bar{n}_2(a+b_2') - \bar{n}_3(a+b_3')}{(n_{20} - n_{30})a}$$

$$(47b) \quad \tan\Theta = \frac{\bar{n}_2 b_2'' - \bar{n}_3 b_3''}{\bar{n}_2(a+b_2') - \bar{n}_3(a+b_3')}$$

A high speed digital computer is used to solve for the \bar{n}_i , b_i' , and b_i'' , in terms of a given set of w_{ij} 's, modulation frequency, and various values of P. Equations (47) are then evaluated and the resulting values for A' and $\tan\Theta$ together

with ω are used in equations (40), (39) and (41) to calculate Z and T_1 . These results can now be compared to values of T_1 calculated from the steady-state saturation equation (43), and also to the time dependence of the return to equilibrium after pulse saturation calculated from equation (18).

V. THE PARAMAGNETIC SALTS.

All the measurements and calculations reported here have been made on the Cr^{3+} ion present as a substitutional impurity in three diamagnetic host lattices, namely aluminum oxide, potassium cobalticyanide and rubidium alum.

In the three host lattices being considered, Cr^{3+} has a ground state degeneracy of four so that the effective spin $S = 3/2$. Its energy states can be described by the following spin Hamiltonian:

$$(48) \quad \mathcal{H} = \beta(g_x H_x S_x + g_y H_y S_y + g_z H_z S_z) + D(S_z^2 - 5/4) + E(S_x^2 - S_y^2)$$

where the nuclear terms have been dropped since their contribution in the salts considered here is quite small.

V.1. Cr^{3+} in Al_2O_3

A trigonal crystalline field gives Cr^{3+} a single orbital ground state, four-fold degenerate as to spin. Spin-orbit interaction partially lifts the degeneracy leaving two two-fold degenerate spin levels, and the application of a dc magnetic field completely removes the degeneracy. The spin Hamiltonian for ruby is circularly symmetric about the z-axis because of the trigonal crystalline field, and is given by equation (48) with $E = 0$.

In the calculations reported here, the values of g and D quoted by Donoho (1964) were used, namely $g=1.980$ (isotropic) and $D=5.733$ Gc/s. Extensive data on the energy levels of ruby have been presented by Chang and Siegman (1958A), and Schulz du Bois (1959).

V.2. Cr³⁺ in K₃Co(CN)₆.

The crystal of K₃Cr(CN)₆ contains two distinct magnetic complexes per unit cell, each consisting of a paramagnetic ion surrounded by a nearly regular octahedron of six CN groups. The two complexes are identical except for the orientation of their axes.

A cubic crystalline field leaves a singlet orbital ground state, four-fold degenerate as to spin. Fields of lower symmetry together with spin-orbit interaction split the ground state into two Kramers doublets.

The energy states of one complex are described by equation (48) with $g=1.992$ (isotropic), $D=0.083 \text{ cm}^{-1}$, and $E=0.011 \text{ cm}^{-1}$ (Bowers and Owen 1955). Extensive data on the energy levels is given by Chang and Siegman (1958B), Butcher (1957) and Weber (1959).

V.3. Cr³⁺ in RbAl(SO₄)₂·12H₂O.

The unit cell of rubidium chrome alum contains four unequivalent complexes whose axes of symmetry are the [111] directions of the cubic crystal. The spin Hamiltonian is circularly symmetric about the z-axis of the complex, and is given by equation (49) with $g=1.975$ (isotropic) and $D=0.342 \text{ cm}^{-1}$ (Vanier 1962).

For all three types of crystal the appropriate spin Hamiltonian was diagonalized and the energy levels and eigenvectors were evaluated on McGill's IBM 7044 computer,

for the particular values and orientations of the dc magnetic field H at which relaxation time measurements were made. The convention adopted for defining the orientation of H is shown in Figure 2 below.

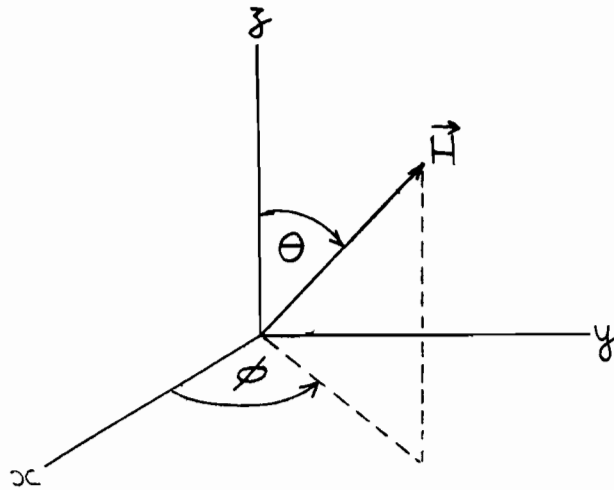


Figure 2.

VI. APPARATUS.

Two spectrometers were used for the measurements reported here. The 890 Mc/s spectrometer, shown in block schematic form in Figure 3, is patterned after apparatus described by Feher (1957) and has been described by Rumin (1961). The modifications necessary to implement the resonance-dispersion technique have been discussed by Carruthers and Rumin (1965).

The main oscillator is a General Radio 1209B. It is free running and has been provided with good temperature lagging, sound insulation, and well-regulated dc supplies for the filament and H.T. currents. The bridge element is a coaxial ring circuit built from modified General Radio 874 components, and is isolated from the main oscillator by means of a 10 dB pad and a 20 dB isolator.

The superheterodyne receiver is linear over the signal range used in the measurements. The balanced detector is a GR 1602B admittance bridge modified to give adequate crystal currents. This drives a balanced I.F.I. P205 preamplifier which is followed by a GR 1216A I.F. amplifier with one stage bypassed and the bandwidth increased from the factory setting.

The high gain audio amplifier uses plug-in twin-T elements to provide narrow-band response at the frequencies used, namely 15, 35, 140 and 400 c/s. A Phazor 200A phase-sensitive detector drives a Texas Servoriter recorder of 5 mV full-scale sensitivity. A conventional phase-shifting circuit, using an RC load on a center-tapped transformer, is placed in

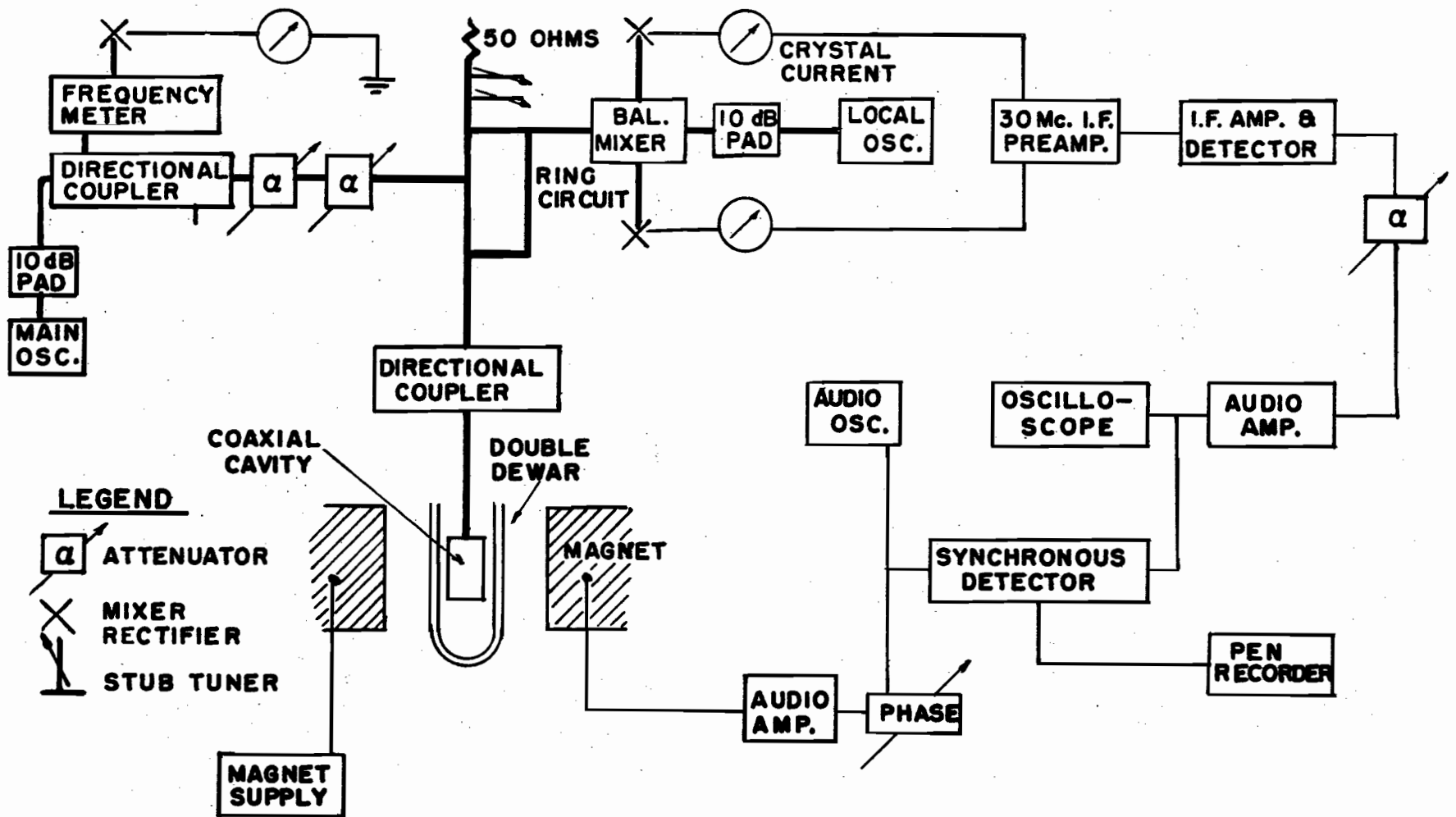


Figure 3. Block schematic of 0.89 Gc/s spectrometer.

the line to the modulating coils to control the phase of the modulating field.

A magnet with 6-inch diameter pole-pieces provides fields up to 2000 oersteds, the stability being one part in 10^4 or better.

A double-dewar system permits operation at liquid Helium temperatures, and facilities have been provided for obtaining lower temperature by pumping over the Helium. A Manostat Corp. Model 8 manostat is used to stabilize the vapour pressure at intermediate points down to 1.6°K which is the lowest attainable temperature.

The 9.4 Gc/s spectrometer has been discussed by Vanier (1962) and is patterned quite closely after apparatus described by Feher (1957). Measurements on this spectrometer were made using the resonance-dispersion technique, and the audio system from the 890 Mc/s spectrometer was utilized for this.

VII. PROCEDURE.

VII.1. Experimental.

All the measurements were made using the resonance-dispersion technique. The procedure is described by Carruthers and Rumin (1965) and more briefly in Chapter IV.

The sample is mounted close to the wall of the coaxial cavity (Rumin 1961) to minimize the curvature of the rf magnetic field lines of force over the sample. For the same reason the sample size is kept quite small. The cavity is not a sealed type so that the crystal is in direct contact with the liquid helium.

The microwave power is initially set to a low level so that saturation effects are negligible. The bridge is adjusted so as to be sensitive to the imaginary component of the incremental susceptibility, $d\chi''$. Any quadrature component present in the audio signal is balanced out by means of the phase-shifting network in the line to the modulation coils. The microwave power is then increased until measurable amounts of saturation and phase-shift are observed. Several measurements are made at different power levels and, where possible, various modulation frequencies. In each case the magnetic field is swept slowly through the line with the synchronous detector switched first to read the real and then the quadrature component. Each measurement is repeated several times.

The attenuation A' and phase angle Θ are obtained by comparing signal intensities at corresponding points,

that is, points equally distant from the center of the line. This procedure is illustrated with the help of Figure 4 below, which shows possible recorder tracings, first for the

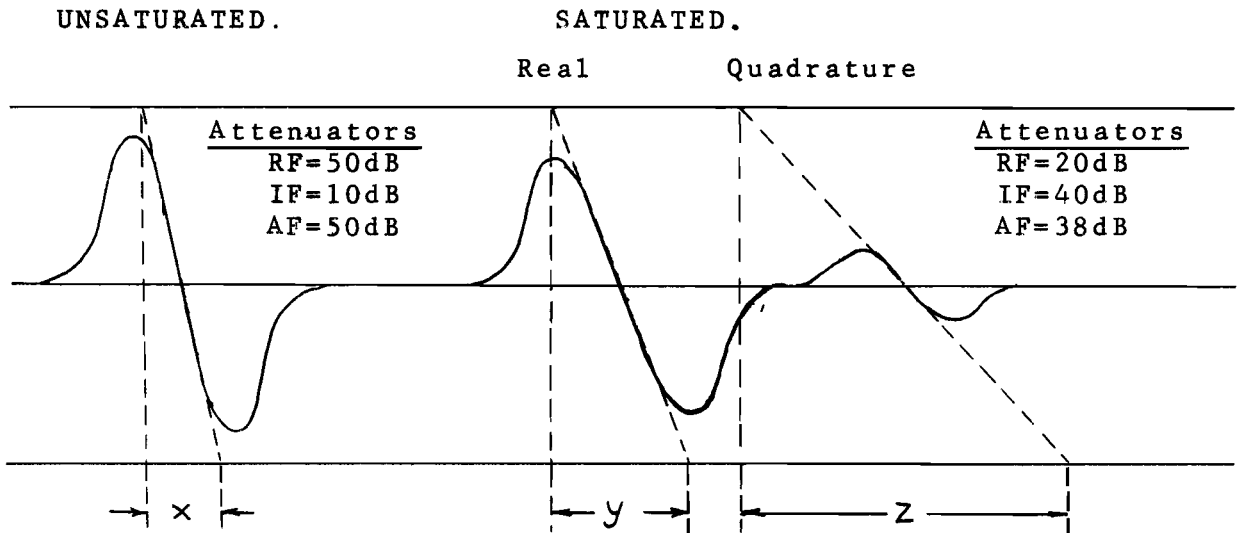


Figure 4

unsaturated line, and then for the real and quadrature components of the partially saturated line. The net change in attenuator settings is evidently 12 dB and, since the derivative of a curve is proportional to its amplitude, it follows that the attenuation A' is given by

$$A' = x / \left[y \left(\text{antilog } \frac{12}{20} \right) \right]$$

and $\tan \Theta$ is

$$\tan \Theta = y/z$$

The values of A' , $\tan \Theta$, and the modulation frequency ω are then used in equations (40), (39), and (41) to determine Z and T_1 .

VII.2. Calculations.

The McGill IBM 7044 computer was used to evaluate the relaxation times that would be yielded by the pulse saturation, resonance-dispersion, and steady-state saturation techniques for the experimental conditions considered. Given the constants of the spin Hamiltonian in equation (48), the magnitude and orientation of the magnetic field H , the temperature T , and the transition to which resonant radiation is applied, the program evaluates the corresponding eigenvalues and eigenvectors of the spin Hamiltonian and calculates the spin-phonon transition probabilities $w_{kk'}$, from equation (11). Actually relative magnitudes of the $w_{kk'}$'s are calculated since no attempt is made to evaluate the constant K'' . The rate equations (17) are then solved, given pulse saturation conditions, and the values of A_1 , A_2 , A_3 and T_1 , T_2 , T_3 in equation (18) are evaluated. The solution is also plotted in semilogarithmic form.

The values of the $w_{kk'}$'s are also fed, together with values of ω , into an auxiliary program which solves for the average steady state populations \bar{n}_i and the real and quadrature components, b_i' and b_i'' , of the time-varying portions of the populations (see Section IV.2). A' and $\tan \Theta$ are evaluated using equations (47), and are then used in equations (40), (39) and (41) to yield the saturation factor Z and relaxation time T_1 that would be obtained from a resonance-dispersion experiment in which the data is processed using an

analysis based on a two-level system.

The populations \bar{n}_i are also used in equation (43), for different values of the radiation induced probability P, to yield the effective $T_1 = 1/2W$ that would be obtained in a steady-state saturation experiment.

Since only relative magnitudes of relaxation times are calculated, in the final analysis the values are normalized to coincide with one experimental point for a given ion and host lattice.

In the case of the pulse saturation calculation, situations arise where the relative magnitudes of the coefficients and time constants of the return-to-equilibrium solution are such that the decay can not be characterized by a single time constant. In such a case the simple exponential solution which "best fits" the decay over approximately two time constants is taken as the effective relaxation time T_R . Figure 5 shows three examples of such a situation.

The complete calculation involving the steps described in the above paragraphs is outlined in Appendix I with the help of a specific numerical example.

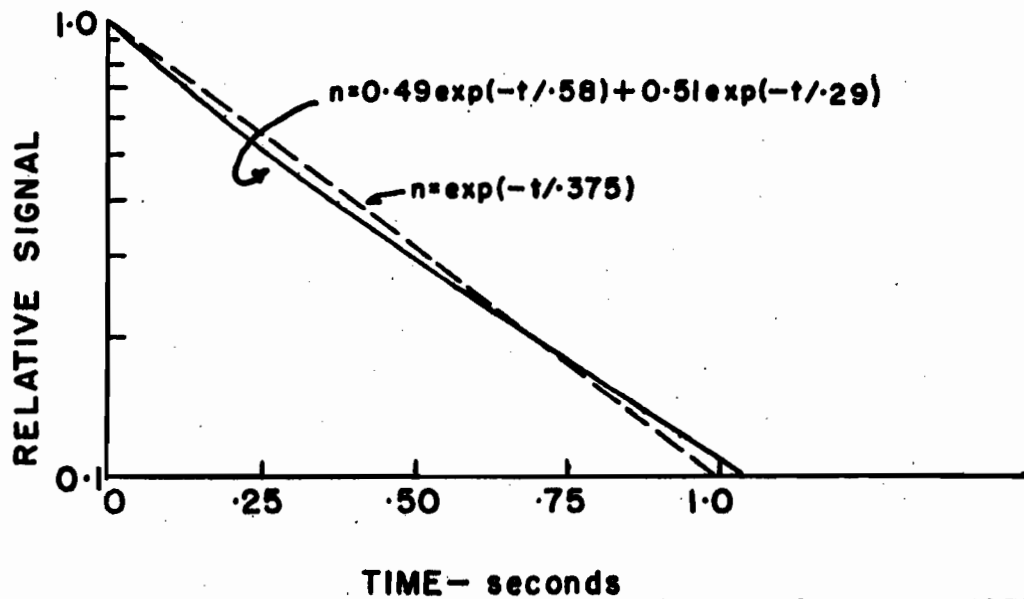
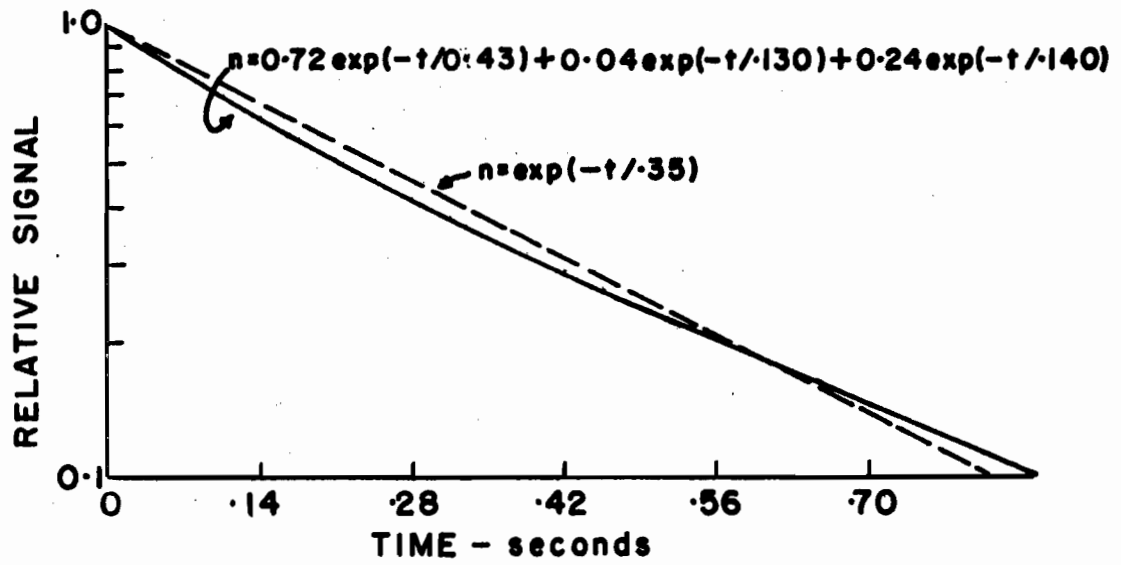
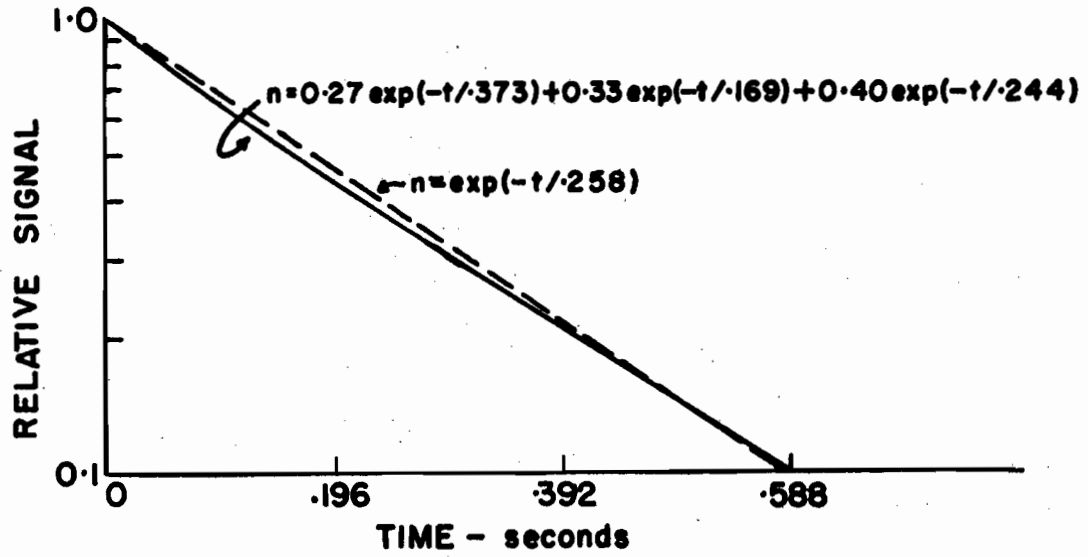


Figure 5. Three examples of calculated decays after pulse saturation. Effective relaxation time T_R is obtained from "best fit" simple exponential shown dotted.

VIII. RESULTS AND DISCUSSION.

VIII.1. Cr³⁺ in K₃Co(CN)₆.

Relaxation times in potassium chromicyanide were measured both at 0.89 Gc/s and at 9.4 Gc/s. Most of the low-frequency measurements were made with the dc magnetic field parallel to the z axis of one of the complexes because under these conditions four transitions are observed over quite a wide range of fields, namely, 105, 340, 1440 and 2050 gauss.* Actually there are six lines since the other complex gives two lines close to the low-field ones. The two lines near 300 gauss are sufficiently far apart that cross-relaxation effects between them were expected to be negligible. But the lines near 100 gauss are improperly resolved and for these measurements the magnetic field was rotated 6 degrees in the ab-plane placing it parallel to the a axis where the energy levels of the two complexes are identical and hence the two lines are superimposed. Since the 100-gauss lines are "radiation forbidden", being (-3/2, 3/2) transitions, the 6dB improvement in signal-to-noise ratio resulting from working with the superimposed lines is quite valuable.

The high-frequency measurements were made on the three radiation-allowed transitions which are observed at 1540, 3360 and 5100 gauss when H is parallel to the axis. Because

*See Figure 8 of Carruthers and Rumin (1965) Appendix II.

Castle et al (1960) and Kipling et al (1961) observed relaxation rates which increased with concentration, an effect not predicted in the theory of spin-lattice relaxation, a dilute crystal was used, namely 0.04% Chromium (the percent concentration being the Cr/Co ratio x 100). Weissfloch* has shown that at this dilution there is negligible concentration dependence for the magnetic field orientation selected.

The results of the high-frequency measurements are shown in Figure 6. As expected the smallest scatter of experimental points was obtained for the 2-3 transition (where the numbering of levels is in order of increasing energy) which is very much stronger than the other two lines. The measurements were made at 4.2°K since Castle et al (1960) and Weissfloch* have shown from an examination of the temperature dependence of the relaxation times that the single-phonon process is dominant at this temperature. For the 2-3 transition a value of 7.6 msec. was obtained, which is in fairly good agreement with Weissfloch's* pulse saturation measurements of 8.2 msec. But the relaxation time for the 3-4 transition (see Table I, page 49) is apparently somewhat higher than Weissfloch's. Since the accuracy of the measurements on the 3-4 transition was quite limited due to the poor signal-to-noise ratio, the actual difference may not be quite as great.

The low-frequency measurements were made on a 0.015%

*C.F. Weissfloch. Private communication.

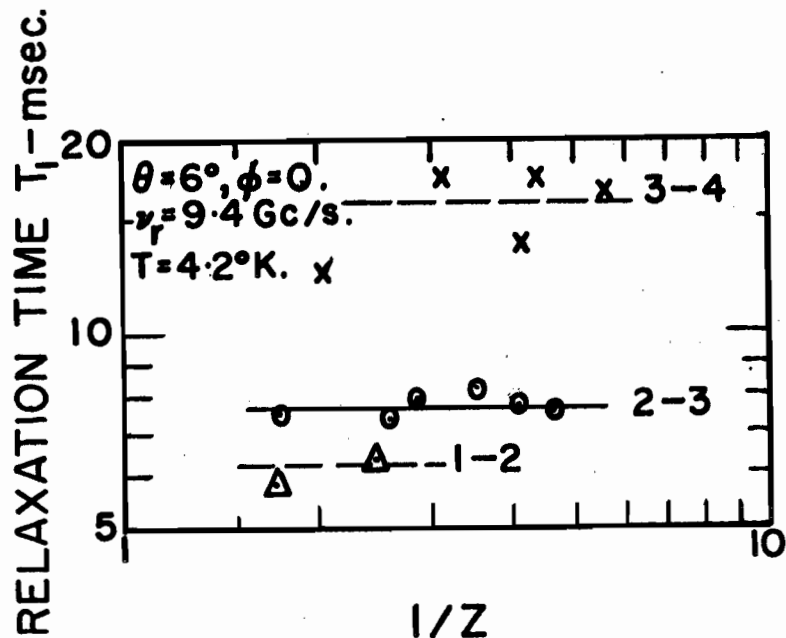


Figure 6. Relaxation times in $\text{K}_3\text{Cr}(\text{CN})_6$ at 9.4 Gc/s and 4.2°K with H parallel to the a-axis. $\omega = 880 \text{ sec}^{-1}$.

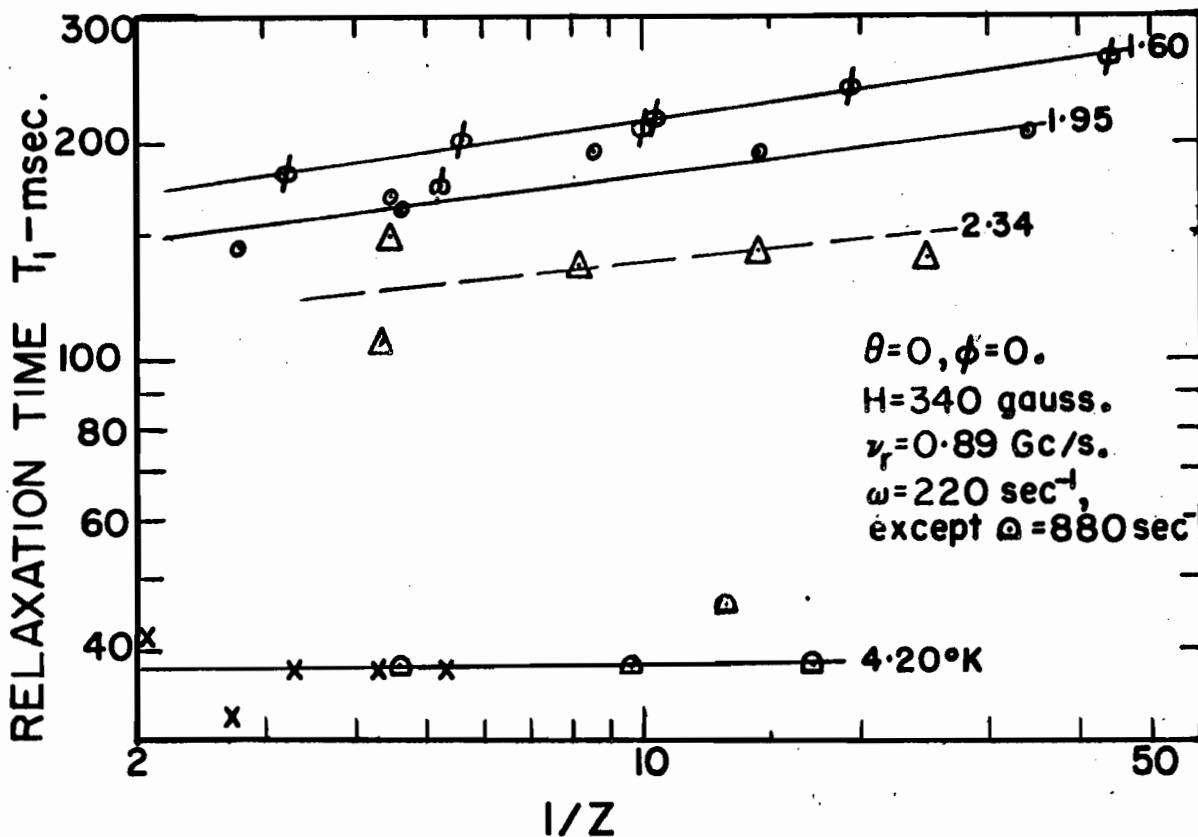


Figure 7. Relaxation times in $\text{K}_3\text{Cr}(\text{CN})_6$ at 0.89 Gc/s for 340 gauss line with H parallel to z-axis. Numbers indicate temperature.

crystal in the case of the 340 gauss line, since Carruthers and Rumin (1965) reported some concentration dependence of the relaxation time still present at 0.06%. The 340 gauss line was sufficiently strong to permit an investigation of the temperature dependence of the relaxation time, and these measurements are shown in Figures 7 and 8. The points which are plotted in Figure 8 were, somewhat arbitrarily, read from the curves in Figure 7 for $1/Z = 10$. It is evident that the relaxation time at 4.2°K varies more rapidly than as $1/T$ suggesting that other relaxation mechanisms besides the single-phonon are operative. Below approximately 2°K the inverse temperature dependence seems to take over.

The slopes in the logarithmic plots of the relaxation time T_1 versus the inverse of the saturation factor Z pose a problem that eludes satisfactory explanation. Carruthers and Rumin (1965) observed similar slopes at 4.2°K which decreased with dilution, and the present measurements at 4.2°K confirm their speculation that the slope would be zero for sufficient dilution with the resultant relaxation time corresponding approximately to the value at which the higher concentration curves intersected. It would seem that the mechanism which produces the slopes at the lower temperatures is different from the one which results in the concentration dependent slopes. This problem will be considered again in a later section.

The other three lines are so much weaker than the 340 gauss transition that for them measurements were made on a

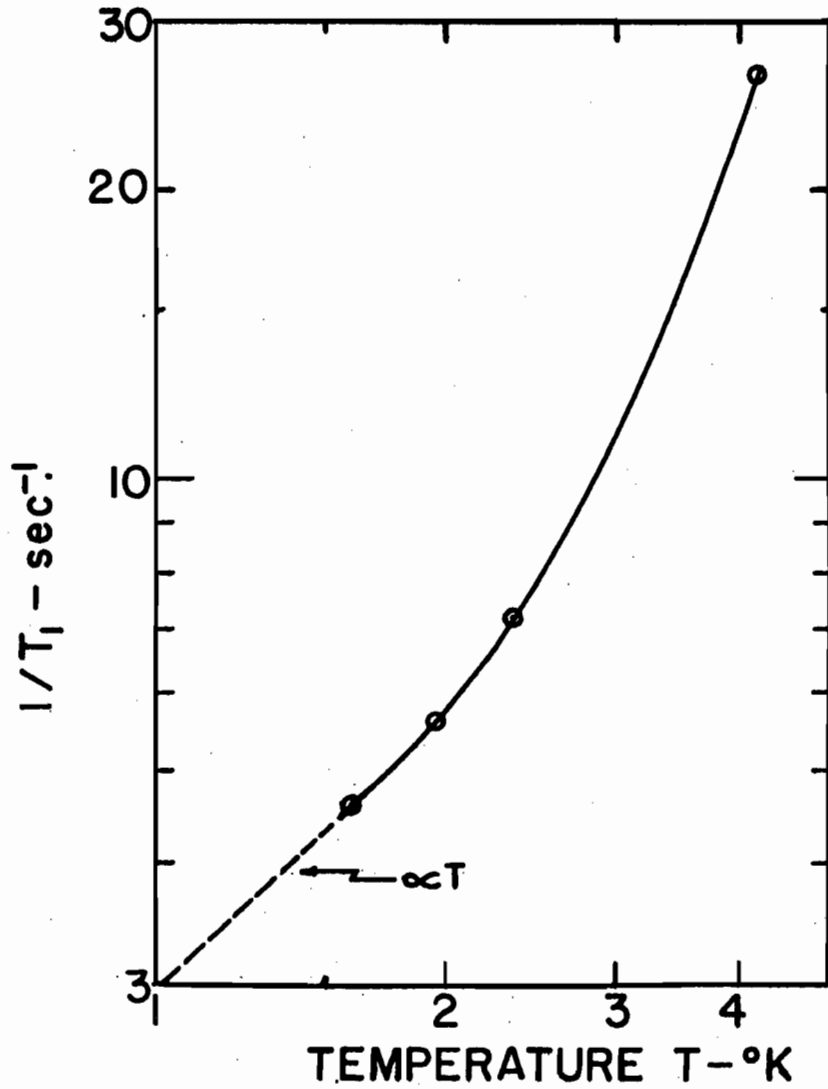


Figure 8. Temperature dependence of relaxation time in $K_3Cr(CN)_6$ at 0.89 Gc/s for 340 gauss line with H parallel to z-axis.

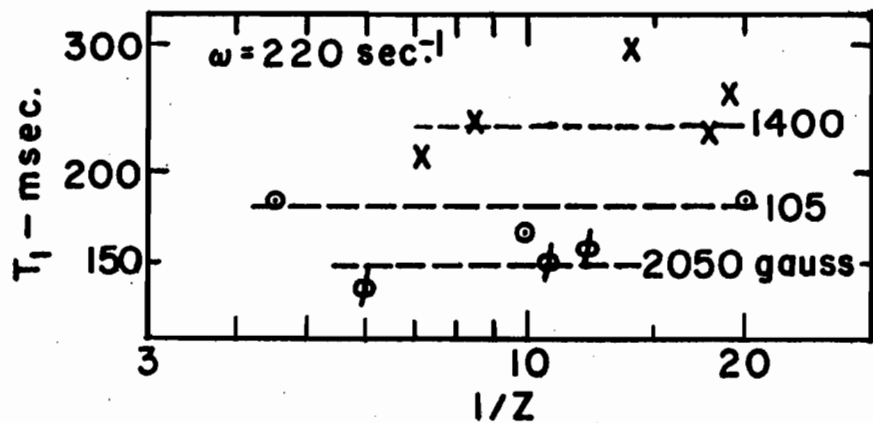


Figure 9. Relaxation times in $K_3Cr(CN)_6$ at 0.89 Gc/s and 1.7°K for 105, 1440, and 2050 gauss lines. H parallel to z-axis except for 105 gauss line parallel to a-axis.

0.06% sample. It was assumed that the temperature dependence of their relaxation times is similar to that of the 340 gauss transition so that the measurements in Figure 9 were also made at a temperature below 2°K.

The results of the above measurements are tabulated in Table I together with other published experimental data on relaxation times in dilute potassium chromicyanide, and the calculated values of the effective relaxation time T_R (see Chapter VII). The calculated values were normalized to coincide with the 9.4 Gc/s pulse saturation measurement for the 2-3 transition corresponding to $\Theta = 6^\circ$, $\phi = 0^\circ$. The normalization is somewhat arbitrary and was chosen mainly because the 2-3 transition at high frequencies is a strong line, and this particular transition has been studied by both the pulse saturation and resonance-dispersion techniques with quite good agreement. Examination of the tabulated data, which, although not by any means comprising an exhaustive study of this salt, nevertheless represents a fair sampling of magnetic fields, orientations and transitions, and a large change in frequency, indicates that the calculations predict the changes in relaxation time to well within a factor of two.

It is interesting to note that the resonance dispersion and the pulse saturation calculations yield relaxation time values which differ by not more than 30%, the pulse saturation values usually being greater. Many of the calculated decay curves had a slight curvature when plotted on semi-logarithmic paper, and, in general, the calculated resonance-

TABLE I

Calculated and Measured Relaxation Times for Cr^{3+}
in $\text{K}_3\text{Co}(\text{CN})_6$ at $T = 1.8^\circ\text{K}$.

Freq.	Field	Angle		Transition	Relaxation Time T_R -msec.			
		θ	ϕ		Resonance-Dispersion		Pulse Saturation	
					Meas.	Calc. ¹	Meas.	Calc. ¹
ν_r	H	deg.	deg.					
Gc/s	Kgauss.	deg.	deg.		Meas.	Calc. ¹	Meas.	Calc. ¹
0.9	0.106	6	0	3-4	170	107		120.
0.9	0.340	0	0	1-2	190	114		127.
0.9	1.440	0	0	1-2	220	195		234.
0.9	2.050	0	0	1-2	140	116		130.
9.4	3.360	6	0	2-3	18 ²	18.9	<u>21.3^a</u>	<u>21.3</u>
9.4	1.540	6	0	3-4	37 ²	22.0	23.5 ^a	29.9
9.4	5.100	6	0	1-2	15 ²	12.2		12.7
9.4	3.2	90	90	2-3		14.0	18.5 ^{2b}	14.1
9.4	3.78	40	90	2-3		15.3	15.5 ^c	14.2

1. Values normalized to coincide with measurement of 2-3 transition for $\nu_r = 9.4$ Gc, $\theta = 6^\circ$, $\phi = 0^\circ$.

2. Extrapolated from 4.2°K measurement assuming inverse temperature dependence.

a. C.F. Weissfloch. Private communication.

b. Kipling, Smith, Vanier and Woonton (1961).

c. Castle, Chester, and Wagner (1960).

dispersion values seem to correspond to the asymptotes to the early portions of these curves. Since the normal range of saturation factors over which resonance-dispersion measurements are made, namely 0.5 - 0.01, represents spin population departures from thermal equilibrium, which in a pulse experiment correspond to points on the decay trace between 0.99 and 0.5 of initial amplitude, it may not be unreasonable to expect smaller values of T_R by the resonance-dispersion technique in cases where the pulse decay exhibits a faster component in the early part of the trace. The last entry in Table I does not seem to fit into this explanation.

VIII 2. Cr³⁺ in Al₂O₃.

At 0.89 Gc/s only one line could be observed in ruby over the range of magnetic fields attainable with the existing magnet power supply. This was the 1-2 transition, situated at approximately 300 gauss when H is parallel to the z axis. The relaxation time was measured on a sample containing approximately 0.006% Chromium* and was found to be 360^{+70} msec. The line is quite weak at this low concentration, resulting in appreciable scatter in the experimental points, but this could not be avoided in view of the concentration dependent relaxation times that have been observed in ruby at higher concentrations (Mims et al 1960). Measurements were made at

*Analyzed by Technical Service Laboratories,
Toronto, Ont.

4.2°K since available data on the temperature dependence of spin-lattice relaxation times in ruby (Feng and Bloembergen 1963, Pace et al 1960) indicated that the single-phonon process would be dominant at this temperature.

The angular dependence of relaxation time was explored on the 9.4 Gc/s spectrometer. A cylindrical sample, 3.2 mm thick and 6 mm in diameter, containing 0.0033% of Chromium,^{*} was used, and the measurements were made at 4.2°K. Figure 10 shows the data obtained at those angles where the transitions studied were strong enough to permit measurement. As in the case of chromicyanide at low temperatures slopes are observed in the logarithmic plots of T_1 against $1/Z$. The fact that the slope seems to be constant for a given transition is noteworthy although not very illuminating.

In an attempt to clarify this problem pulse saturation measurements were made with C.F. Weissfloch on his 9.2 Gc/s spectrometer. For angular variations close to the z axis usable measurements were obtained only for the 2-3 transition^{**} at $\Theta = 20^\circ$ where an essentially single exponential decay with a time constant of 180 msec. was observed. This corresponds to resonance-dispersion measurements at a saturation factor Z of approximately 0.1.

* Analyzed by Bell Telephone Laboratories, Inc., Murray Hill, N.J.

** For many angles there are two 2-3 transitions in ruby at 9.2 Gc/s, one at low fields and one at high fields, and, unless otherwise noted, the high field one will be understood.

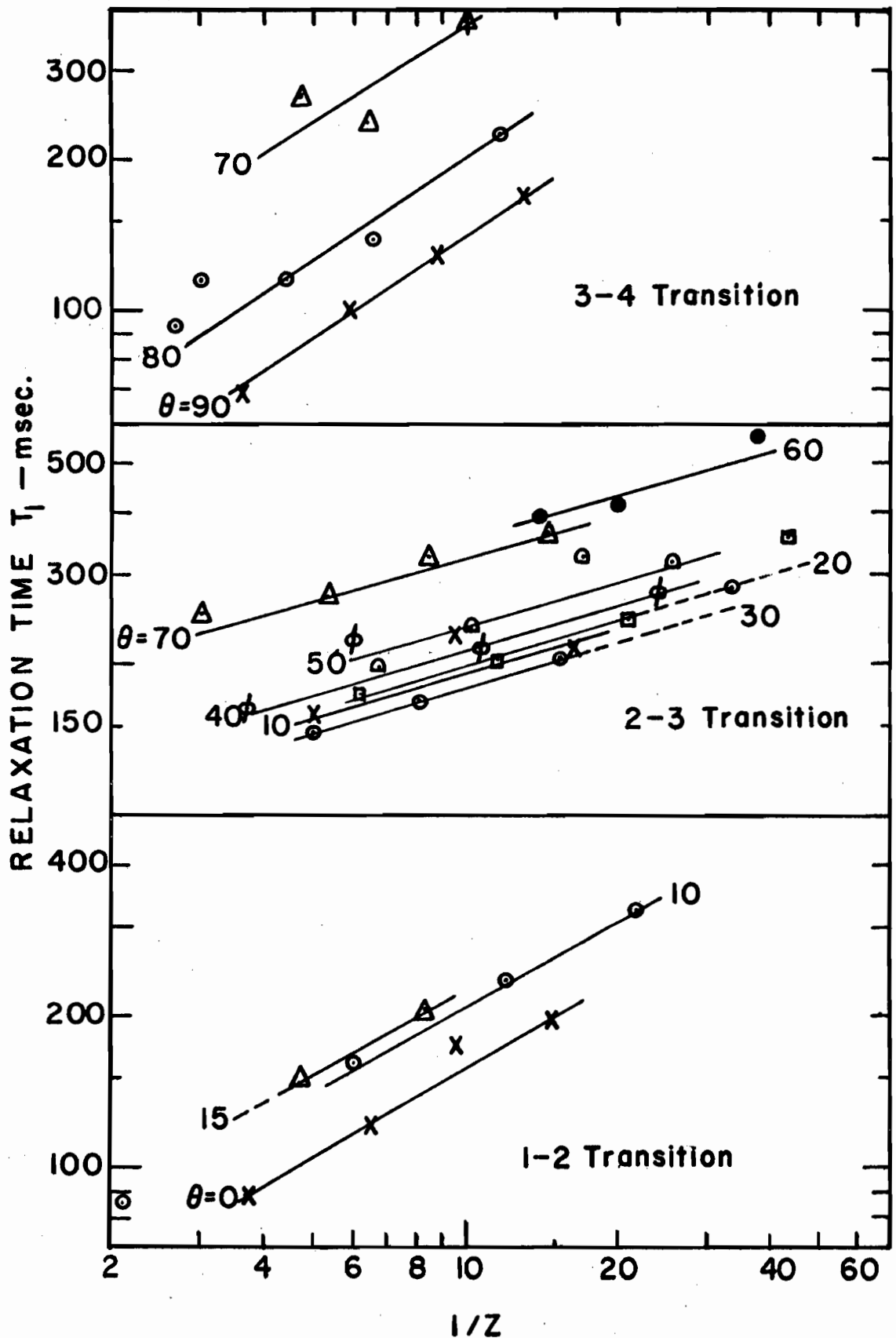


Figure 10. Relaxation times in uncut ruby crystal at 9.4 Gc/s and 4.2°K. Numbers indicate angle of H with z-axis. $\omega = 220 \text{ sec}^{-1}$.

With the possibility of the slopes being caused by a phonon bottleneck in mind, the crystal was cut in half perpendicular to its flat face, and resonance-dispersion measurements were repeated for a few orientations. Some of the results of these measurements are presented in Figure 11. In general the data were quite poor, to a large extent due to the smaller sample. Nevertheless, the results are good enough to suggest that the measured relaxation times T_1 are not functions of the degree of saturation, and correspond to the values obtained at the highest values of $1/Z$ on the large sample.

Since Weissfloch's pulse saturation measurements on the uncut sample were obtained at the limit of the spectrometer's sensitivity, no attempt was made to determine whether decays with larger time constants would be observed with the smaller crystal.

Using the measurements on the smaller sample as a basis, values of T_1 were read from Figure 10, corresponding to $1/Z = 10$ for the 1-2 transition, $1/Z = 40$ for the 2-3, and $1/Z = 20$ for the 3-4 transition, and were plotted as a function of the angle Θ . The results are plotted in Figures 12 and 13, together with the effective relaxation times T_R for pulse saturation conditions calculated following the procedure discussed in Chapter VII. Making use of experimental data on the spin-lattice interaction Hamiltonian for ruby, Donoho (1964) calculated the w_{ij} 's and hence the parameters of the decay equation (18). His calculations, just as

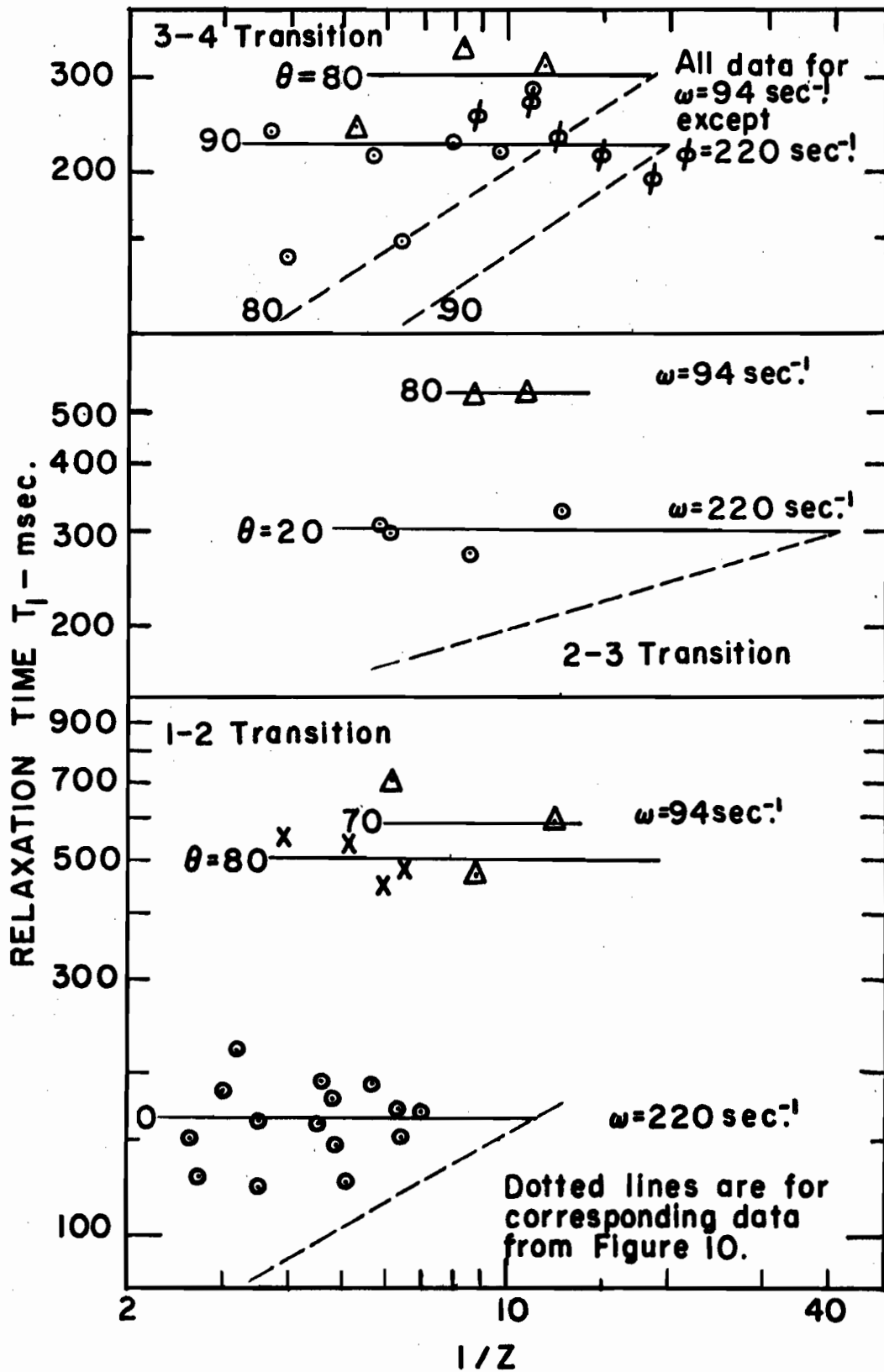


Figure 11. Relaxation times in small ruby crystal at 9.4 Gc/s and 4.2°K. Numbers indicate angle of H with z-axis.

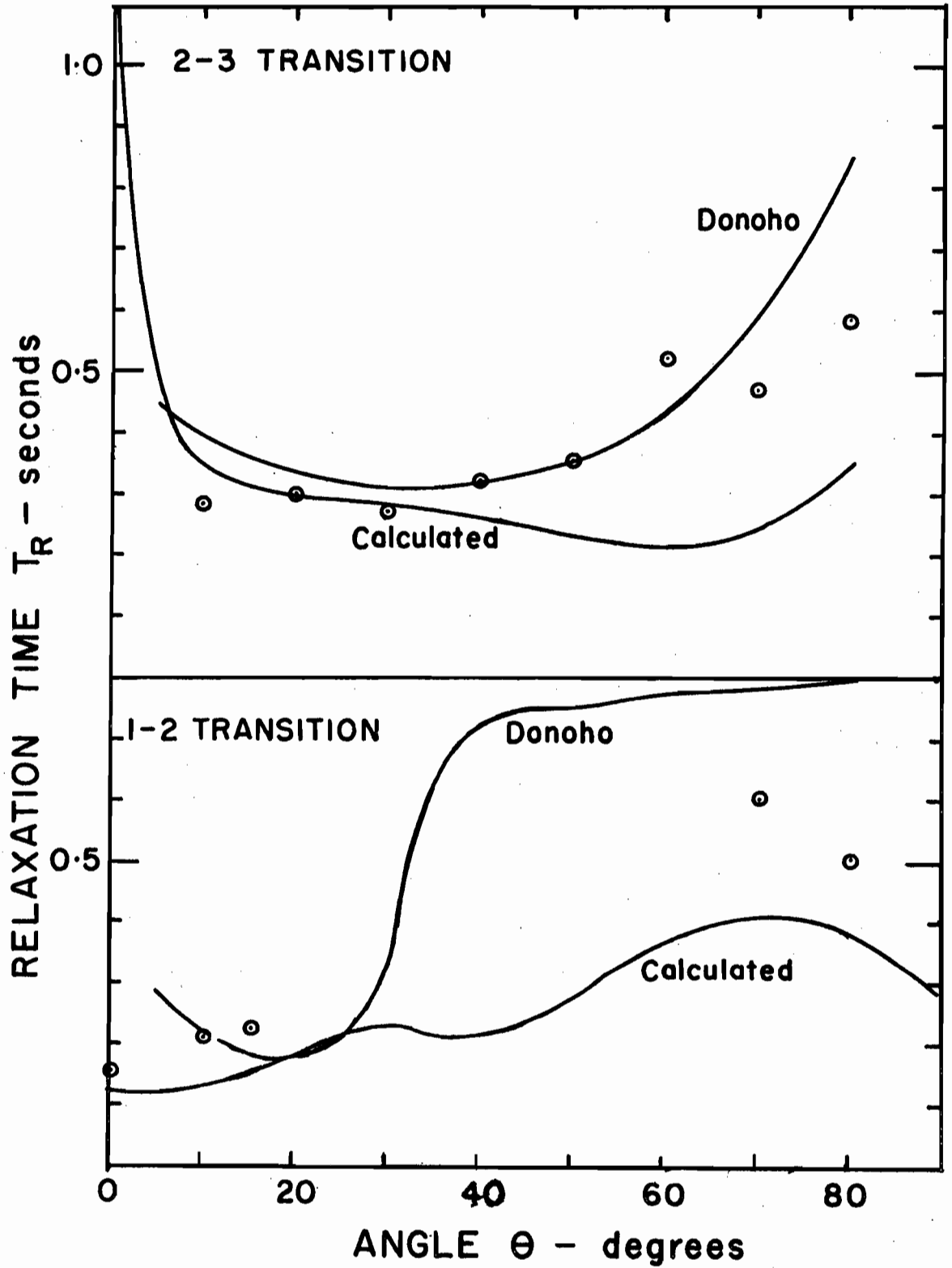


Figure 12. Angular dependence of relaxation times in ruby at 9.4 Gc/s and 4.2°K for 1-2 and 2-3 transitions. Circled points are measured values taken from Figures 10 and 11.

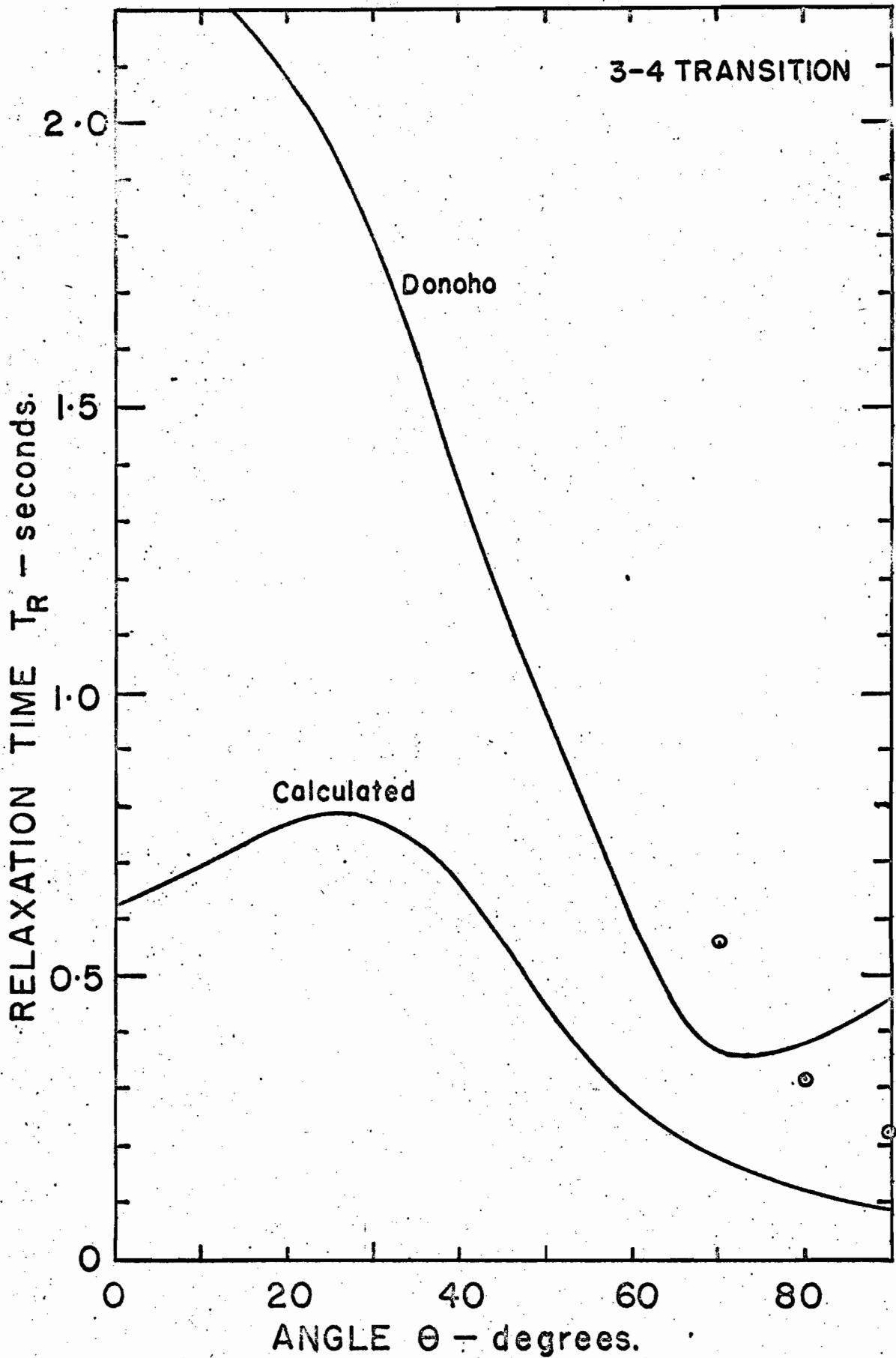


Figure 13. Angular dependence of relaxation time in ruby at 9.4 Gc/s and 4.2°K for 3-4 transition. Circled points are measured values taken from Figures 10 and 11.

those reported here, show that in general one time constant, usually the largest one, dominates the form of the return to equilibrium. Consequently, his data have also been used to compute the resulting decay curves which were then fitted with single exponentials as discussed in Chapter VII. The results of these calculations appear in Figures 12 and 13. No normalization was required for Donoho's results since he calculated the complete w_{ij} 's but the results of the present calculations were normalized to coincide with the measured data for the 2-3 transition at $\Theta = 20^\circ$.

The curves calculated on the basis of equation (11) agree with Donoho's insofar as the general trend of the angular dependence is concerned. Thus both calculations predict for the 1-2 transition longer relaxation times around $\Theta = 90^\circ$ than around $\Theta = 0^\circ$, and vice versa for the 3-4 transition. In the case of the 2-3 transition Donoho's results seem to predict a little better the relative change of relaxation time with Θ . For the other two transitions the experimental data is rather limited but it is interesting that, as the calculations predict, the relaxation time for the 3-4 transition does increase when H is rotated away from $\Theta = 90^\circ$, and in the case of the 1-2 transition the relaxation times are appreciable longer near $\Theta = 90^\circ$ than around $\Theta = 0^\circ$.

Measurements of relaxation times for ruby at several frequencies have been reported. Those which were made at paramagnetic ion dilutions sufficient to minimize concentration

effects are tabulated in Table II together with Donoho's results and the calculations of this author. Of the measurements reported here only the 0.89 Gc/s one and a randomly selected point from Figure 12 are included. The present calculations seem to predict the changes in relaxation time about as well as Donoho's*. Once again the resonance-dispersion calculations yield relaxation times somewhat shorter than those calculated for pulse saturation conditions. This is particularly noticeable for the 2.9 Gc/s case where there was appreciable departure from simple exponential behavior in the calculated decay curve.

Pace et al (1960) measured the relaxation times of the several transitions that can be observed in ruby with $\nu_r = 34.6$ Gc/s and $\Theta = 90^\circ$. Thus both frequency and orientation were kept constant. Table III shows their results for two temperatures at which the measurements indicated that the single-phonon process was dominant, together with

*The results of Donoho's calculations were taken from his Table I which serves the same purpose as our Table II. In the case of the 9.3 Gc/s data for the 2-3 transition at $\Theta = 54^\circ$ it was possible to also make use of his Figure 3 which shows the angular dependence of the parameters of the return-to-equilibrium equation (18). This is a particularly simple case since one time constant wholly dominates the decay for all values of Θ . It is clear from those curves that T_R is approximately 0.38 sec. and not the 0.226^R sec. shown in Donoho's table which, to the accuracy with which the graphs can be read, is the value of one of the other time constants. There is also some disagreement

the calculated values which were normalized in the same way as those in Table II. The predicted changes in relaxation time on the whole seem to be in quite fair agreement with experiment. It should be noted however that while the calculations seem to predict a diminishing temperature dependence at higher fields, the measured relaxation times vary approximately as T^{-1} even at 14.5 Kgauss. With $\nu_r = 34.6$ Gc/s and $T = 4.2^\circ\text{K}$ or less, the high temperature approximation $h\nu \ll kT$, on the basis of which the inverse temperature dependence of the spin-phonon transition probability is predicted, becomes quite poor, and for sufficiently high frequencies and/or low temperatures, w_{ij} and w_{ji} do not vary in the same way (equation 11). Because of this and the fact that we are dealing here with multiple relaxation paths, it is not easy to predict the behavior of the effective relaxation time with temperature. More high frequency and low temperature measurements are needed to decide whether the rather poor agreement for the 14.5 Kgauss line is meaningful or not.

*(continued from previous page)

between Table II and Donoho's Table I in the designation of transitions. For example, his Table I identifies the 7.2 Gc/s entry as a 2-3 transition at 80° which is surprising in view of what Mims et al (1960) report, and because according to Donoho's convention of numbering levels the 2-3 gap never becomes as small as 7.2 Gc/s at $\theta = 80^\circ$. Attempts to clear up these points by communication with Donoho have elicited no response. It is believed that the data presented in Table II is consistent with what has been reported by the authors of the various measurements, in the light of the convention adopted here of numbering levels with increasing energy.

TABLE II

Calculated and Measured Relaxation Times for Cr³⁺
in Al₂O₃ at 4.2°K.

Freq. ν_r Gc/s	Field H Kgauss	Angle θ deg.	Tran- sition	Relaxation Time T _R -sec.				
				Resonance- Dispersion		Pulse Saturation		
				Meas.	Calc.*	Meas.	Calc.*	Donoho
34.6	7.0	90	2-4		0.033	0.054 ^a	0.034	0.080
9.3	4.0	54	2-3		0.188	<u>0.20</u> ^b	<u>0.200</u>	0.226
9.4	7.5	0	1-2	0.15	0.105		0.115	
9.2	4.3	20	2-3		0.252	0.18 ^c	0.280	
7.2	1.4	90	1-2		0.314	0.50 ^d	0.343	0.539
2.9	0.6	60	1-2		0.672	0.50 ^e	0.920	0.750
0.9	0.3	0	1-2	0.36	0.358		0.390	

* - Values normalized to coincide with pulse measurement for 9.3 Gc/s, $\theta = 54^\circ$.

a - Pace, Sampson and Thorp (1960).

b - Nisida (1962).

c - C.F. Weissfloch. Private communication.

d - Mims and McGee (1960).

e - Armstrong and Szabo (1960).

TABLE III

Comparison of Pulse Saturation Measurements and Calculations of Relaxation Times for Cr^{3+} in Al_2O_3 at $T=1.4$ & 4.2°K , $\theta=90^\circ$, and $\nu_r=34.6$ Gc/s.

Field H Kgauss	Transition	Relaxation Time T_R -msec			
		$T=4.2^\circ\text{K}$		$T=1.4^\circ\text{K}$	
		Meas. ^a	Calc.*	Meas. ^a	Calc.*
3.8	1-4	-	-	296	256.
4.8	1-3	56	45.2	100	117.
7.0	2-4	54	33.5	147	83.8
10.0	1-2	22	23.6	59	69.4
12.3	2-3	16	17.5	64	42.4
14.5	3-4	21	13.5	60	16.7

*-Same normalization as in Table II.

a-Pace, Sampson and Thorp (1960).

VIII.3. Cr^{3+} in $\text{RbAl}(\text{SO}_4)_2 \cdot 12\text{H}_2\text{O}$.

Resonance-dispersion measurements were made at 0.89 Gc/s on a rubidium alum crystal containing approximately 0.03% Chromium. For most orientations the lines due to the four complexes are clustered within a range of magnetic fields between approximately 50 and 400 gauss, and are either improperly resolved or are situated sufficiently close together that the presence of cross-relaxation may not be ignored. However, when the magnetic field is directed parallel to the z axis of any one complex a transition is observed at

approximately 1100 gauss. The results of measurements on this line are presented in Figure 14. Once again slopes in the T_1 versus $1/Z$ plots complicate the picture. The factor of ten change in T_1 between 4.2°K and 1.97°K suggests that at the higher temperature other mechanisms besides the single-phonon one are operative. At the lower temperatures the scatter of the experimental points prevents a decision on the exact nature of the temperature dependence, although it is not likely to be much faster than T^{-1} .

At X-band the relaxation time of the 2-3 transition has been measured by Dyment (1965) as a function of temperature, and by Vanier (1962) at 4.2°K . In view of the temperature dependence at 0.89 Gc/s, Dyment's results are used in the comparison of experimental and calculated values shown in Table IV.

TABLE IV

Calculated and Measured Relaxation Times for Cr^{3+}
in $\text{RbAl}(\text{SO}_4)_2 \cdot 12\text{H}_2\text{O}$ at $T=1.95\text{K}$.

Freq.	Field	Angle	Trans'n	Relaxation Time T_R -msec			
				Resonance-Dispersion		Pulse Saturation	
				Gc/s	Kgauss	deg	Meas.
9.4	3.375	90	2-3		9.4	<u>10^a</u>	<u>10</u>
0.9	1.065	0	1-2	150	220.		250

* - Values normalized to coincide with pulse measurement at 9.4 Gc/s.

a - Dyment (1965).

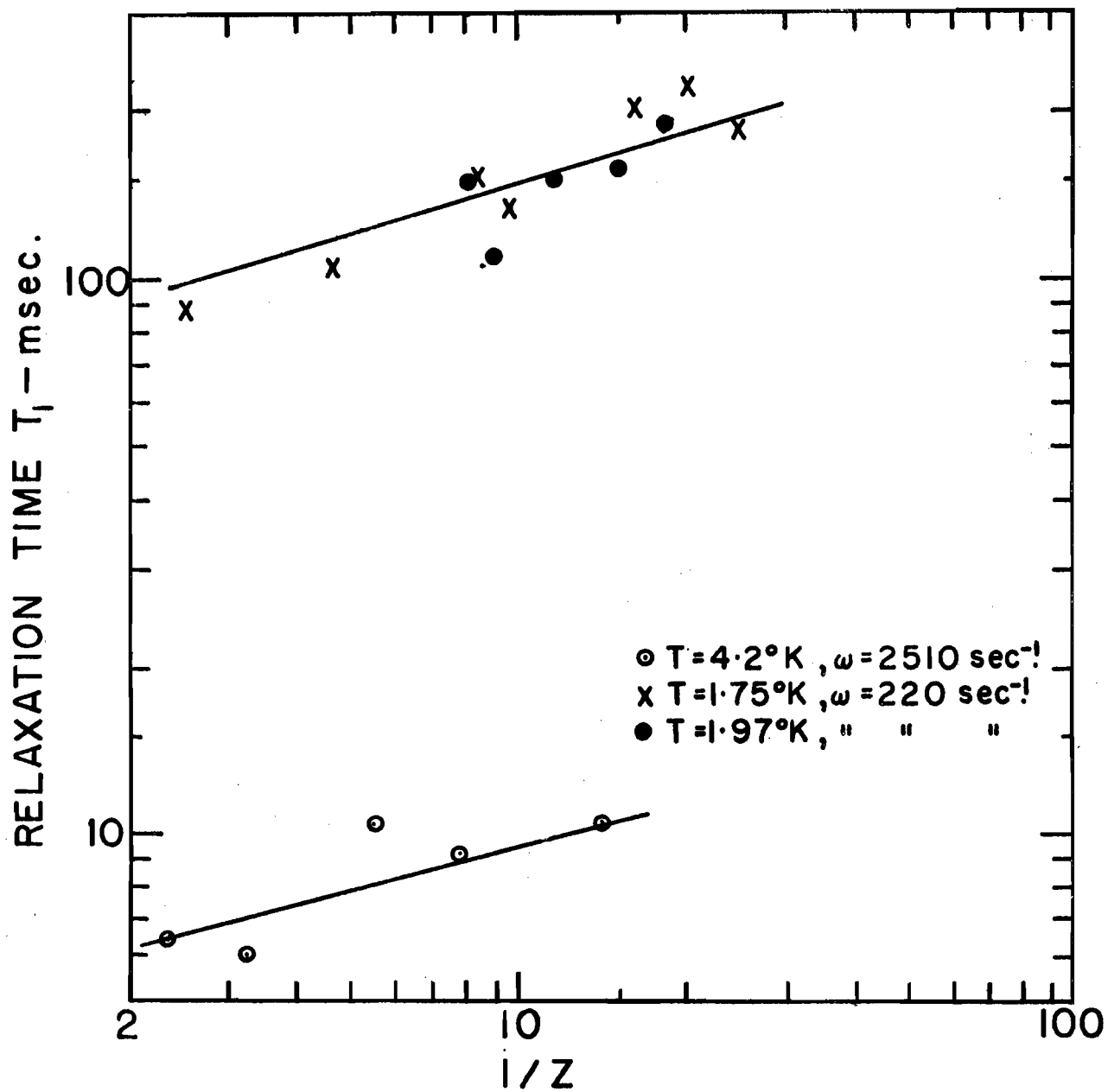


Figure 14. Relaxation times in $\text{RbCr}(\text{SO}_4)_2 \cdot 12\text{H}_2\text{O}$ at 0.89 Gc/s for 1100 gauss line with H parallel to z-axis.

As in the case of chromicyanide the value of T_1 corresponding to $1/Z=10$ was read from the graph in Figure 14, and the calculated values were normalized to coincide with the X-band measurement of the 2-3 transition.

Measurements on one or two of the lines at low fields yielded times that were as much as an order of magnitude shorter than predicted by the calculations, adding some support to the assumption that cross-relaxation mechanisms were operative between those closely spaced lines.

VIII.4. The Slopes in the Logarithmic Plots of T_1 versus $1/Z$.

An important point which emerges from the resonance-dispersion calculations is that even in cases where there is relatively severe departure from simple exponential behavior of the calculated pulse saturation decay, the relaxation time T_1 is constant for modulation frequencies and saturation factors down to those satisfying the expression $\omega T_1 Z=1$ (see Chapter IV). On the basis of these calculations one would not expect the slopes in the logarithmic plots of T_1 versus $1/Z$ that have been observed for so many of the measurements reported here.

No satisfactory explanation for the variation of T_1 with Z has been arrived at from a consideration of both some known physical processes which may be operative at the concentrations and temperatures of interest, and the possibility of the effect being instrumental. For example, the order of magnitude

equation given by Giordomaine and Nash (1965) for predicting the occurrence of a phonon bottleneck indicates that this phenomenon is extremely unlikely with the experimental conditions and results reported here. Although a size dependence of relaxation time may be associated with a phonon bottleneck it is felt that the measurements on ruby, when size is reduced, are inconclusive.

The effects of cross-relaxation were also considered as a possible explanation for the dependence of T_1 on Z . Bloembergen et al (1959) discuss the case of a lattice with N_α ions with two energy levels separated by $h\nu_\alpha$ and N_β ions with two energy levels separated by $h\nu_\beta$, where $\nu_\alpha - \nu_\beta \ll \nu_\alpha$. Assuming for simplicity that $N_\alpha = N_\beta$, their rate equations (14) were simplified (Weissfloch, 1964) and solved on a high-speed computer for the case of an applied rf field at the frequency ν_α , in a manner similar to that used for resonance-dispersion calculations for a multi-level system (see Chapter VII). This was done for a range of the two spin-lattice relaxation times T_α and T_β , the cross-relaxation time T_{21} , and modulation frequency ω . Although $T_1 = T_\alpha$ was found to increase with $1/Z$ whenever T_{21} was shorter than T_α , the results were very strongly dependent on modulation frequency, an effect which was not observed in the present measurements (see, for example, results for 3-4 transition in Figure 11). To the extent that a multi-level system can be looked upon as behaving like a two-level one, the above model does not explain the observed variation of T_1 with Z . Nor does it, one might add,

explain the concentration dependent slopes observed by Carruthers and Rumin (1965).

The cross-relaxation model described above was also used as a basis for investigating the effect of spin diffusion in a manner similar to that suggested by Bloembergen et al (1959). The resonance line was simulated by four equally populated, two-level spin systems having identical spin-lattice relaxation times but different cross-relaxation times. As before the results showed appreciable dependence of T_1 on $1/Z$ but again a very strong modulation frequency effect.

The failure to explain the slopes thus leaves unanswered the question of how to determine the spin-lattice relaxation time from the experimental data. However, because in most cases the relaxation time T_1 changes by a factor of only approximately two in going from large to small Z , the general conclusions that are drawn from the measurements are not greatly affected by how one selects a relaxation time from a given plot of T_1 versus $1/Z$, providing one is consistent from then on. Thus, for example, the conclusions regarding the angular dependence in ruby are not significantly affected by whether one selects the relative values of T_1 by the method adopted, or by reading values of T_1 from Figure 10 corresponding to a fixed, arbitrarily selected value of $1/Z$, or even by taking averages of T_1 over the appropriate range of saturation factors.

VIII.5. Calculations for Steady State Saturation Conditions.

As mentioned in Chapter VII, calculations were made of the effective relaxation time that a steady-state saturation measurement would yield. Since none of the experimental data considered here were obtained by this technique, the results of these calculations were not included in the preceding sections of this chapter. For every experimental point considered the calculations yielded identical values of relaxation time for the resonance-dispersion and steady-state saturation conditions. Since the rate equations were solved for selected values of the radiation-induced transition probability P , none of the difficulties which the experimentalist encounters in the calculation of P ever arose.

IX. CONCLUSIONS

The following results emerge from the work reported here:

1) The relative magnitudes of the $S(2S + 1)$ spin-phonon transition probabilities between the $2S + 1$ levels of the $S = 3/2$ ion Cr^{3+} in $\text{K}_3\text{Co}(\text{CN})_6$, Al_2O_3 , and $\text{RbAl}(\text{SO}_4)_2 \cdot 12\text{H}_2\text{O}$ are approximately determined, for the single-phonon relaxation process (equation 11), by:

a) the quadratic spin operator matrix elements, and
b) the temperature and frequency dependent terms, namely the Debye equation (7), the Bose-Einstein factor, and the $\nu^{1/2}$ in equation (5) which appears in the coefficients of the expansion of the crystalline field potential in normal lattice modes. The relative changes in the effective spin-lattice relaxation time with the magnitude and direction of the dc magnetic field, frequency, and temperature are predicted, on the basis of such a simplified theory, with an accuracy that is usually better and rarely worse than a factor of two. There seems to be no reason why the above simplifications can not be generalized to any spin system of $S > 1/2$.

2) Although in the recently proposed resonance-dispersion technique the experimental data is processed by an analysis based on a two-level system, calculations indicate that for a multi-level system the measured single-phonon, spin-lattice relaxation time T_1 should be constant for all modulation frequencies ω and saturation factors Z down to those

satisfying the expression $\omega T_1 Z \approx 1$. Furthermore, it should be equal to the value obtained by the pulse saturation method if the decay is essentially a simple exponential. Where there is appreciable departure from single-time-constant behavior the resonance-dispersion value is still independent of ω and Z but is better approximated by the time constant obtained from the asymptote to the early portion of the decay's semi-logarithmic plot. Calculations also indicate that in both cases discussed above the steady-steady saturation technique should yield results identical to those of the resonance-dispersion method.

3) Relaxation times have been measured at both 0.89 Gc/s and 9.4 Gc/s by the resonance-dispersion technique. The low-frequency measurements constitute, to the best of the author's knowledge, the first paramagnetic resonance measurements on dilute crystals of potassium chromicyanide, ruby, and rubidium chrome alum at a frequency an order of magnitude lower than the X-band where most measurements have been made*, and at a temperature low enough to ensure that the single-phonon relaxation mechanism was dominant. The measurements at X-band have shown the feasibility of using the resonance-dispersion technique at this frequency and, in the case of

* Van Vleck (1961) reports briefly on frequency dependence measurements on potassium chromicyanide, but no numerical details of the measurements are given nor have they apparently been published elsewhere.

potassium chromicyanide, have confirmed that the spin-lattice relaxation times measured by both this and the pulse saturation method should be equal if the pulse measurement exhibits simple exponential behavior. It is believed that the measurements on ruby represent the first reported systematic investigation of the angular dependence of spin-lattice relaxation times in crystals of extremely low Chromium concentration. For reasons mentioned below the measurements sometimes introduce some uncertainty into the determination of the relaxation time but the general trend is in agreement with the calculations reported here and the more exact ones made by Donoho (1964).

4) In many cases the interpretation of measurements has been complicated by an apparent slight dependence of the relaxation time T_1 on the saturation factor Z , resulting in T_1 at the smallest values of Z where measurements could be made being approximately twice the value obtained at the largest values of Z . A satisfactory explanation for this effect has not been found. No similar effect has apparently been reported for pulse-saturation measurements on very dilute crystals. The reason for this may be that in the resonance-dispersion technique, measurements are made on transitions between levels whose populations have been severely disturbed by continuous resonant radiation, while in the pulse technique the effective relaxation time is read off that portion of the decay which corresponds to relatively light disturbances of populations returning to thermal equilibrium some time after the removal of resonant radiation.

5) Experimental confirmation has been obtained for the speculation by Carruthers and Rumin (1965) that the concentration-dependent slopes in the logarithmic plot of T_1 versus $1/Z$, which they observed at 0.89 Gc/s and 4.2°K in potassium chromicyanide, would tend to zero at sufficiently low Cr^{3+} concentration, with the resultant T_1 being approximately equal to the value obtained corresponding to the smallest Z .

BIBLIOGRAPHY

- Andrew, E.R. 1956. Nuclear magnetic resonance (Cambridge University Press, London and New York).
- Andrew, E.R. and Tunstall, D.P. 1961. Proc. Phys. Soc. (London) 78, 1
- Armstrong, R.A. and Szabo, A. 1960 Can. J. Phys. 38, 1304.
- Bloemberger, N., Purcell, E.M., and Pound, R.V. 1948. Phys. Rev. 73, 679.
- Bloembergen, N., Shapiro, S., Pershan, P.S., and Artman, S.O. 1959. Phys. Rev. 114, 445.
- Bloembergen, N. and Pershan, P.S. 1961. Advances in quantum electronics, edited by Jay R. Singer (Columbia University Press, London and New York), p. 373.
- Bowers, K.D. and Owen, J. 1955. Reports on Progress in Physics, 18, 304.
- Bowers, K.D. and Mims, W.B. 1959. Phys. Rev. 115, 285.
- Butcher, P.N. 1957. Electron Tube Laboratory Tech. Rept. No. 155-1, Stanford Electronics Labs., Stanford, California.
- Carruthers, J.A. and Rumin, N.C. 1965. Can. J. Phys. 43, 576.
- Castle, J.G., Chester, P.F., and Wagner, P.E. 1960. Phys. Rev. 119, 953.
- Chang, W.S. and Siegman, A.E., 1958, Electron Tube Laboratory Tech. Repts. Nos. (A) 156-1, (B) 156-2, Standford Electronics Labs., Stanford, California.
- Cole, K.S. and Cole, R.H. 1941. J. Chem. Phys. 9, 341.
- Davids, D A. and Wagner, P.E. 1964. Phys. Rev. Letters, 12, 141.
- Donoho, P.L. 1964. Phys. Rev. 133, A1080.
- Dyment, J.C. 1965. Ph.D. Thesis, Department of Physics, McGill University, Montreal (unpublished).
- Feher, G. 1957. Bell System Tech. J. 36, 449.
- Feng, S. and Bloembergen, N. 1963. Phys. Rev. 130, 531.

- Gill, J.C. and Elliot, R.J. 1961. Advances in quantum electronics, edited by Jay R. Singer (Columbia University Press, London and New York), p. 399.
- Gill, J.C. 1962. Proc. Phys. Soc. (London) 79, 58.
- Giordomaine, J.A. and Nash, F.R. 1965. Phys. Rev. 138, A1510.
- Gorter, C.J. 1947. Paramagnetic relaxation (Elsevier Publishing Company Inc., Amsterdam).
- Kipling, A.L., Smith, P.W., Vanier, J., and Woonton, G.A. 1961. Can. J. Phys. 39, 1859.
- Kronig, R. de L. 1939. Physica, 6, 33.
- Lloyd, J.P. and Pake, G.E. 1954. Phys. Rev. 94, 579.
- Mattuck, R.D. and Strandberg, M.W.P. 1960. Phys. Rev. 119, 1204.
- Mims, W.B. and McGee, J.D. 1960. Phys. Rev. 119, 1233.
- Nisida, Y. 1962. J. Phys. Soc. (Japan) 17, 1519.
- Pace, J.H., Sampson, D.F. and Thorp, J.S. 1960. Proc. Phys. Soc. (London) 76, 697.
- Paxman, D.H. 1960. Rept. No. 364, Mullard Research Labs.
- Rannestad, A. and Wagner, P. 1963. Phys. Rev. 131, 1953.
- Rumin, N.C. 1961. M.Sc. Thesis, Department of Physics, McGill University, Montreal (unpublished).
- Scott, P.L. and Jeffries, C.D. 1962. Phys. Rev. 127, 32.
- Schulz du Bois, E.O. 1959. Bell System Tech. J. 38, 271.
- Vanier, J. 1962. Ph.D. Thesis, Department of Physics, McGill University, Montreal (unpublished).
- Van Vleck, J. H. 1940. Phys. Rev. 57, 426.
- Van Vleck, J.H. 1961. Advances in quantum electronics, edited by Jay R. Singer (Columbia University Press, London and New York) p. 388.
- Waller, I. 1932. Z. Physik, 79, 370.

Weber, J. 1959. Rev. Mod. Phys. 31, 681.

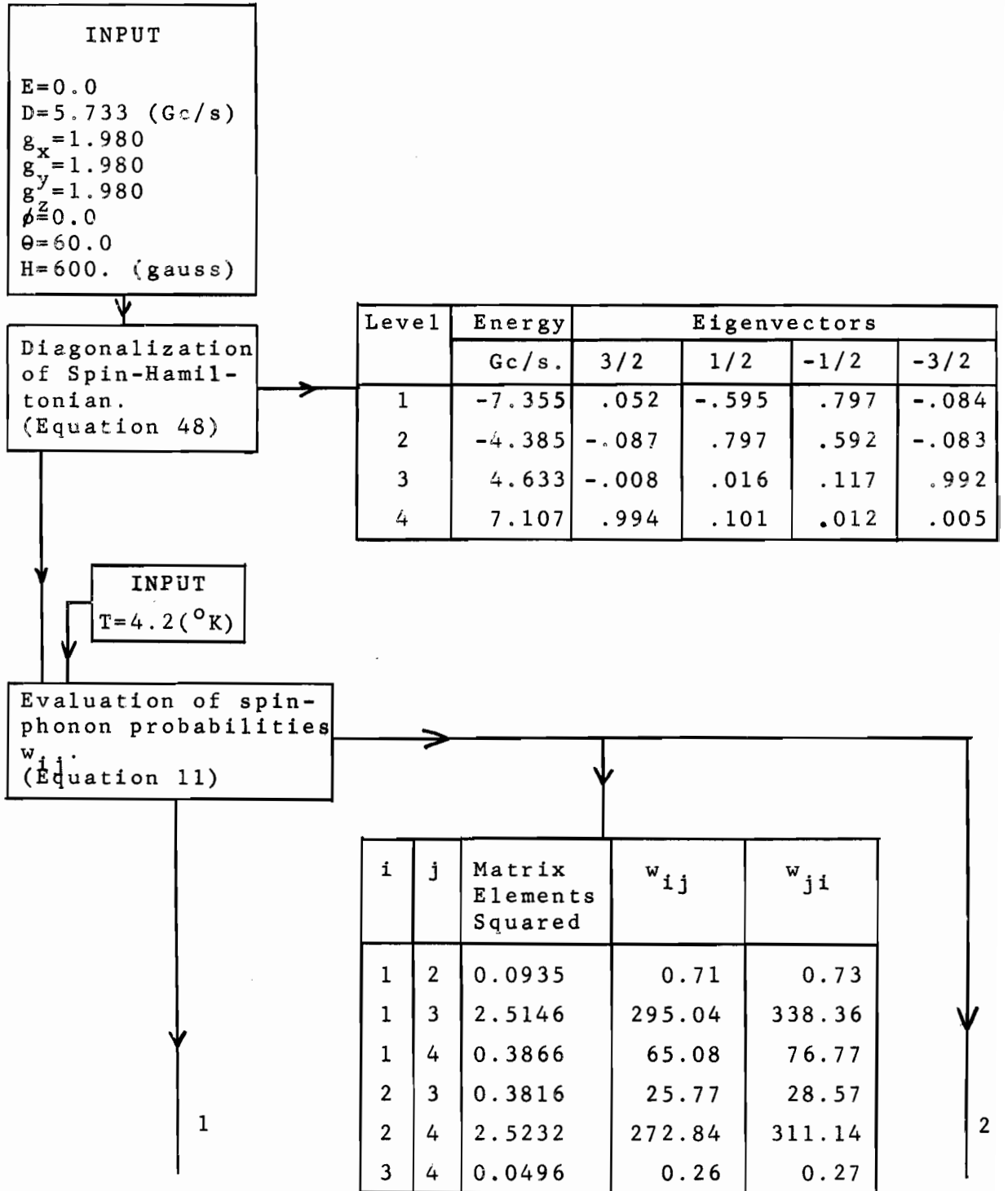
Weissfloch, C.F. 1964. M.Sc. Thesis, Department of Physics,
McGill University, Montreal (unpublished).

Woonton, G.A. 1961. Advances in electronics and electron
physics, edited by L. Marton (Academic Press, N.Y.)
p.163.

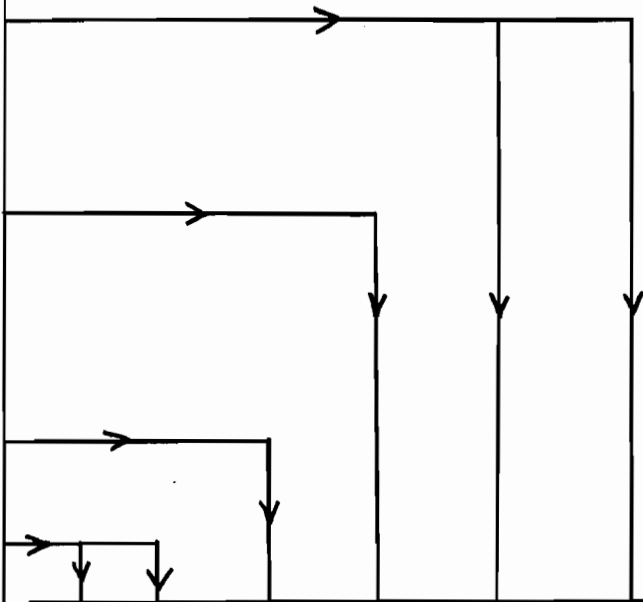
APPENDIX I.

Calculation of Relaxation Times.

Example. Relaxation time of 1-2 transition in ruby for $H=600$ gauss, $\theta=60^\circ$, $T=4.2^\circ\text{K}$.



1	2
<p>Operation on equation (17), (modified by equations (26) and (42), and with w_{12} and w_{21} replaced by w_{12}^{21+P} and w_{21}^{12+P}), namely:</p> <p>1) Steady-state portion solved for \bar{n}_i.</p> <p>2) $T_R = 1/2W$ solved for from equation (43).</p> <p>3) Time dependent portion solved for b'_i and b''_i.</p> <p>Solution of equations (47) for A' and $\tan \theta$.</p> <p>Solution of equations (40), (39), and (41) for Z and T_1.</p>	



$\omega = 220 \text{ sec}^{-1}$					
T_1	Z	$\tan \theta$	T_R	$\frac{n_1 - n_2}{n_{10} - n_{20}}$	P
sec			sec		sec ⁻¹
.673	.189	.029	.672	.189	3.2
.673	.104	.058	.672	.104	6.4
.673	.055	.116	.672	.055	12.8
.674	.028	.232	.672	.028	25.6
$\omega = 440 \text{ sec}^{-1}$					
.672	.189	.014	.672	.189	3.2
.672	.104	.029	.672	.104	6.4
.672	.055	.058	.672	.055	12.8
.673	.028	.116	.672	.028	25.6
$\omega = 880 \text{ sec}^{-1}$					
.672	.189	.007	.672	.189	3.2
.672	.104	.014	.672	.104	6.4
.672	.055	.029	.672	.055	12.8
.672	.028	.058	.672	.028	25.6

APPENDIX II

MEASUREMENT OF SPIN-LATTICE RELAXATION AT 890 Mc/s
BY A RESONANCE-DISPERSION TECHNIQUE.

J.A. Carruthers and N.C. Rumin.

Canadian Journal of Physics, Volume 43 (April, 1965)

MEASUREMENT OF SPIN-LATTICE RELAXATION AT 890 Mc/s
BY A RESONANCE-DISPERSION TECHNIQUE

J. A. CARRUTHERS AND N. C. RUMIN

MEASUREMENT OF SPIN-LATTICE RELAXATION AT 890 Mc/s BY A RESONANCE-DISPERSION TECHNIQUE

J. A. CARRUTHERS¹ AND N. C. RUMIN

Eaton Electronics Research Laboratory, McGill University, Montreal, Quebec

Received November 30, 1964

ABSTRACT

A new technique has been used to measure the spin-lattice relaxation time of Cr^{+++} in $\text{K}_3\text{Co}(\text{CN})_6$ at 890 Mc/s. The method depends on observing both the amplitude and phase of the audio signal developed at the modulation frequency in a bridge-type microwave resonance spectrometer. One or more modulation frequencies are used, depending on the value of the relaxation time and the degree of saturation employed. Although similar to the saturation technique, this method does not require knowledge of the power level or the linewidth, and is suited to measurements on weak lines. Results have been obtained for lines at 100, 300, 1 400, and 2 100 oersteds, using crystals containing 0.06% and 0.4% chromium. The values of T_1 for the lower concentration are in the 20–30-millisecond range, but relaxation appears to be not equivalent to a single time-constant. For the higher concentration the relaxation times are shorter and there is a marked evidence of multiple time-constants.

1. INTRODUCTION

Measurements on paramagnetic relaxation in recent years have emphasized the microwave resonant approach, using either the saturation method or the pulse technique. The audio-frequency relaxation method, used mainly by the Leyden group, dates to a much earlier time (Waller 1932; Gorter 1947). The technique described here is similar to both the microwave saturation method and the audio-frequency relaxation approach. The dispersion of the incremental susceptibility at audio modulation frequencies is observed at various levels of saturation, produced by resonance absorption at the microwave frequency. The dispersion observed can be related to the spin-lattice relaxation time by extending the saturation theory to include the effect of fluctuating spin populations during the modulation cycle.

Values of relaxation time (T_1) obtained by various techniques have shown inconsistencies and have not fitted well into a general theory (Van Vleck 1960). Until recently the theories of the interaction between the electron spins and the crystal lattice have been based on two mechanisms, a direct process in which a spin absorbs (or emits) a phonon of energy equal to that of the spin transition, and a Raman process in which one phonon may be absorbed and another emitted at a different frequency. An example of the changeover from the Raman to the direct process is reported by Paxman (1960) for $\text{K}_3\text{Fe}^{3+}(\text{CN})_6$ as the temperature is lowered from 4.2 °K to 1.6 °K. Bloembergen, Shapiro, Pershan, and Artman (1959), in reporting the effects of cross relaxation, have helped to point out the reason for some of the inconsistencies. In addition, Bloembergen and Pershan (1961), Van Vleck (1961), and Gill and Elliot (1961) have recently extended this concept to excited states.

¹Present address: Department of Electrical Engineering, University of Minnesota, Minneapolis, Minnesota, U.S.A.

The present experiments were undertaken in order to determine the value of T_1 for $K_3Cr(CN)_6$ at a frequency lower than those previously reported. Van Vleck (1961) has pointed out that the values obtained at 10 cm, 3 cm, and 8 mm are in approximate agreement with a $1/f^2$ frequency dependence, so that by working at 890 Mc/s one could obtain a check on this law.

The theory of microwave saturation in a paramagnetic sample is reviewed briefly and then extended to include the dispersion effects which are observed at the modulation frequency. Use is made of the concept of an equivalent conductance mesh in order to help in the visualization of the saturation and relaxation mechanisms.

2. REVIEW OF SATURATION THEORY

Two papers (Lloyd and Pake 1954; Kipling *et al.* 1961) give detailed developments of the theory of saturation in paramagnetic resonance, and only a brief review is included here. Where possible, the expressions are simplified by the use of constants of proportionality since the technique described in the later sections depends only on relative signal intensities, not on absolute values.

If the population of spin state j in a multilevel system is n_j^0 at thermal equilibrium, and is n_j when partially saturated, the saturation factor S_{jk} for the transition between the j and k levels is given by

$$(1) \quad S_{jk} = (n_k - n_j)/(n_k^0 - n_j^0).$$

The rate equations which describe the changing population densities can be written as:

$$(2) \quad dn_j/dt = \sum_k (n_k W_{kj} - n_j W_{jk}).$$

The total transition probability W_{jk} from level j to level k is the sum of the phonon-induced probability w_{jk} and the radiation-induced probability V_{jk} . The values of w_{jk} and w_{kj} are related by the Boltzmann factor corresponding to the energy difference between the two levels. The radiation-induced probabilities are reversible so that $V_{jk} = V_{kj}$.

When radiation acts on a particular pair of levels long enough for steady-state conditions to be established, the system can be described as having reached a stationary state, but this does not correspond to thermal equilibrium. The rate equations have $dn_j/dt = 0$ and hence for stationary conditions

$$(3) \quad \sum_k (n_k W_{kj} - n_j W_{jk}) = 0.$$

In experimental work the microwave radiation is applied between a particular pair of levels, and the radiation-induced probability is zero except for this transition. The subscripts on V are therefore unnecessary and are omitted to simplify terminology. Similarly, the symbol S , without subscripts, refers to the saturation factor for this same pair of levels. The net effective relaxation probability from the upper to the lower of these two states includes the effect of relaxation by way of the other levels, and is given the symbol W .

Lloyd and Pake (1954) show that the saturation factor in the presence of radiation is given by

$$(4) \quad S = (1 + V/W)^{-1},$$

and W can be written, for the 1-2 transition, in the form,

$$(5) \quad W = w_{21} + C_{21}^{-1} \sum_{k=3}^n w_{2k} C_{2k}.$$

The expressions for the cofactors C_{jk} are given in the original paper, but are not included here. In spite of the complexity of equation (5), the representation of the net effective relaxation probability is fairly simple if one works with the equivalent passive network of conductances. The equivalent mesh for a four-level system is shown in Fig. 1, where each node point corresponds to one of

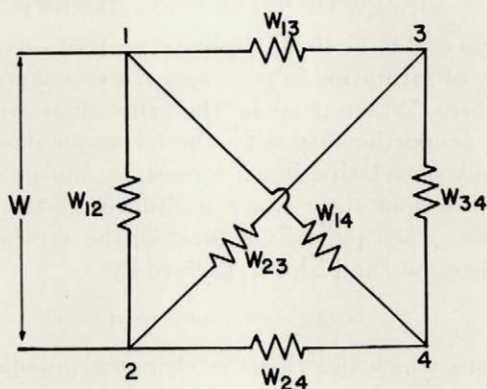


FIG. 1. The equivalent conductance mesh for a four-level system determining the net effective relaxation probability W in terms of the phonon-induced probabilities w_{jk} .

the energy levels of the system, and each individual conductance is the corresponding phonon-induced relaxation probability w_{jk} . To be more precise, one should use in the equivalent mesh the mean of w_{jk} and w_{kj} , but at 4.2 °K and 890 Mc/s these two terms are different by only about 1%, and the error involved in neglecting this difference is not significant.

It is worth noting that the equivalent-circuit concept can be useful in calculating the saturation factor S . In the series circuit of Fig. 2, consisting of

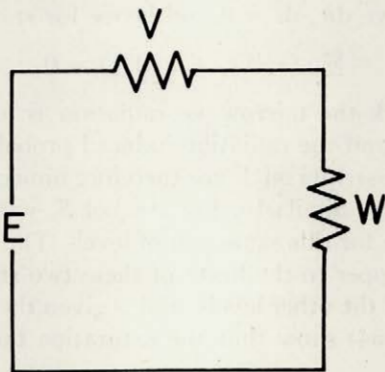


FIG. 2. The equivalent circuit for calculating S from the radiation-induced probability V and the net relaxation probability W . The value of S is given by $(1 + V/W)^{-1}$, which is the ratio of the voltage across V to the total voltage E .

the radiation-induced probability V , the relaxation probability W , and a series e.m.f. E , the value of S given by equation (4) is the ratio of the voltage across V to the source voltage. The analogy between a partially saturated system and an active mesh is found to be of general value in analyzing the behavior of the system and is further developed in Section 7.

The objective in saturation measurements is to determine the relaxation probability W . It follows from equation (4) that the value of W can be determined from measurements which determine S as a function of V , and this procedure is the basis of the saturation technique. The spin-lattice relaxation time T_1 is related to W , for a simple two-level system, by

$$(6) \quad T_1 = 1/2W.$$

Even in multilevel systems, in which it may not be possible to describe the relaxation process by a single time-constant, it is common practice to define T_1 by equation (6).

The experimental measurements are based on determining the power absorbed in the paramagnetic sample as a function of the incident power. If we arbitrarily designate the levels between which the radiation acts as levels 1 and 2, the expression for the power absorbed per unit volume of the sample is given by

$$(7) \quad P = (n_2 - n_1)\nu hV.$$

From the definition of the saturation factor, equation (7) can be written as

$$(8) \quad P = S(n_2^0 - n_1^0)\nu hV.$$

But the power absorbed can also be expressed in terms of the imaginary part of the magnetic susceptibility, χ'' , and the microwave magnetic field strength, H_1 :

$$(9) \quad P = 4\pi\nu\chi''H_1^2.$$

From equations (8) and (9),

$$(10) \quad \chi'' = [S(n_2^0 - n_1^0)hV]/4\pi H_1^2.$$

The actual value of V depends on many factors, including the orientation of the crystal with respect to the steady magnetic field. But since the dispersion technique developed in Sections 3-6 does not require knowledge of the absolute magnitude of V , we shall write it merely as being proportional to $H_1^2g(\nu)$, where $g(\nu)$ is the line-shape factor defined by

$$(11) \quad \int_0^\infty g(\nu)d\nu = 1: \\ V = JH_1^2g(\nu).$$

Combining equations (10) and (11), and introducing a new constant of proportionality K , we have

$$(12) \quad \chi'' = KSg(\nu),$$

where

$$K = [(n_2^0 - n_1^0)hJ]/4\pi.$$

For measurements of the relaxation probability W by the saturation technique, only relative values of χ'' are important. From equation (9) χ'' is seen to be proportional to the ratio of the power absorbed to the power incident, and the change in this ratio, as saturation occurs, is all that needs to be measured. The saturation factor S can be determined experimentally for particular values of input power, and using equations (4) and (11) the relaxation probability can be calculated. The conventional saturation technique therefore requires accurate knowledge of the radiation-induced probability V , and thus J , H_1 , and $g(\nu)$ must be known. One advantage of the resonance-dispersion method described in later sections is that these quantities do not appear explicitly in the final equations.

In practice it is customary to use frequency or magnetic field modulation and synchronous detection in order to obtain a better signal-to-noise ratio. Modulation of the magnetic field is the preferred approach because extraneous reflections in the microwave system can cause difficulty when frequency modulation is employed. The magnetic field H is modulated at an audio frequency ω while H is slowly swept through the line. The amplitude of modulation is small compared to the linewidth and the curve traced out on the recorder is proportional to the slope of the χ'' versus H plot. We are therefore interested in an expression for the differential of χ'' , which can be obtained from equation (12). But when H is varied instead of the frequency ν , the line-shape factor in equations (11) and (12) will be written as $g(H)$, where

$$\int_0^{\infty} g(H)dH = 1.$$

Therefore, we have

$$(13) \quad d\chi'' = K(Sdg(H) + g(H)dS).$$

Equation (13) is the basis of measurements of relaxation probability by the saturation technique when low-level modulation of the magnetic field is employed. As discussed by Bloembergen *et al.* (1948) and Andrew (1956), there are two conditions under which this equation can be put in a simple enough form for reduction of experimental data.

Case (1). When the magnetic field is modulated at a rate which is very slow compared to the relaxation probability, the spin populations readjust quickly enough during the modulation cycle for us to assume that stationary conditions apply at all times. Equations (4) and (11) can be used to express dS in terms of $dg(H)$. Therefore, at very low modulation frequencies,

$$(14a) \quad d\chi'' = KS^2dg(H).$$

Case (2). When the modulation rate is very fast compared to the relaxation probability, the spin population can be assumed to be constant during the modulation cycle. Hence dS can be put equal to zero and we have

$$(14b) \quad d\chi'' = KSdg(H).$$

Equations (14a) and (14b) show that if H is set at some arbitrary point of a

partially saturated line and the modulation frequency is slowly varied, a form of dispersion should be observed with the signal at a very high frequency, greater than that at very low frequency by the factor $1/S$. This dispersion, illustrated qualitatively in Fig. 3, results because the spin-lattice relaxation

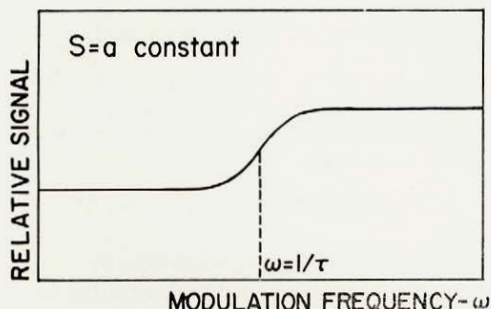


FIG. 3. Qualitative dispersion curve showing the increase in signal as the modulation frequency is increased.

probability is comparable to the modulation rate over a particular range of modulation frequencies.

In conventional measurements using the saturation technique it is important to choose a modulation frequency such that dispersion is not present. But, as shown by Bloembergen *et al.* (1959) and Andrew (1956), the effective value of relaxation time when radiation is applied is ST_1 , not T_1 . The region of dispersion therefore shifts to higher frequencies as the saturation factor decreases, and the choice of modulation frequency for performing experiments on a sample which has T_1 equal to several milliseconds is a serious practical problem.

In the sections which follow, the dispersion region is examined more fully in order to show how the effect can be used to advantage in measurements of spin-lattice relaxation time.

3. THE DISPERSION EQUATIONS

In order to obtain equations which describe the region of dispersion it is necessary to go back to the rate equations. Stationary conditions are not applicable, and the fluctuations in the spin populations during the modulation cycle must be taken into account. The additional complexity involved in dealing with nonstationary conditions has resulted in our being able to obtain a solution for a two-level system only. However, the results of Castle *et al.* (1960) show that it is often a very good approximation to assume that a single-valued relaxation time occurs for the four-level Cr^{3+} ion in dilute crystals of $\text{K}_3\text{Cr}(\text{CN})_6$. In this case it would appear difficult to distinguish between relaxation occurring between the two levels directly, and relaxation by way of the other two levels. Consequently, the solution of the two-level case should be of interest, at least as a first step.

If the upper and lower of the two levels are designated 1 and 2 respectively, the rate equations become

$$dn_1/dt = n_2W_{21} - n_1W_{12},$$

$$dn_2/dt = n_1W_{12} - n_2W_{21},$$

using the relation $w_{12} = w_{21}e^{h\nu/kT}$, and letting w be the mean of w_{21} and w_{12} , we have, to good approximation,

$$W_{12} = w(1 + h\nu/2kT) + V,$$

$$W_{21} = w(1 - h\nu/2kT) + V.$$

By subtracting the two rate equations, and using the condition that $n_1 + n_2 = N$, the total ion density, we obtain

$$d(n_2 - n_1)/dt = 2w(Nh\nu/2kT - (n_2 - n_1)) - 2(n_2 - n_1)V.$$

If we let n represent the population difference, $n_2 - n_1$, and let n_0 be the difference at thermal equilibrium, the rate equation becomes

$$(15) \quad dn/dt = 2w(n_0 - n) - 2nV.$$

When sinusoidal modulation is applied to the magnetic field, the line-shape factor $g(H)$ is caused to fluctuate. If the amplitude of modulation is small compared to the linewidth, the $g(H)$ term will be sine-wave modulated. The expression for V can therefore be written in terms of a mean value V and a small component which varies at the modulation frequency ω :

$$V = \bar{V}(1 + ae^{j\omega t}).$$

We assume a solution for n of the same form as for V ,

$$n = \bar{n}(1 + be^{j\omega t}).$$

Substitution for n and V in equation (15) yields

$$(16) \quad 2n_0w = \bar{n}(2w + 2\bar{V}) + e^{j\omega t}(2w\bar{n}b + j\omega\bar{n}b + 2\bar{n}\bar{V}b + 2\bar{n}\bar{V}a) + 2\bar{n}\bar{V}abe^{j2\omega t}.$$

The last term is very small and, being at twice the modulation frequency, it will be rejected by the synchronous detector. Equation (16) can then be separated into two parts, one involving the mean values, the other containing the time-varying terms:

$$(17a) \quad \bar{n}/n_0 = (1 + \bar{V}/w)^{-1},$$

$$(17b) \quad \bar{n}b(2w + j\omega)e^{j\omega t} + 2\bar{n}\bar{V}(a + b)e^{j\omega t} = 0.$$

The first part of equation (17) gives the mean value of the saturation factor during the modulation cycle, and is given the symbol S :

$$(18) \quad S = (1 + \bar{V}/w)^{-1}.$$

Equation (17b) involves the amplitudes of the alternating components and hence must contain information on the dispersion. But to use this equation for experimental determinations of w it is necessary to interpret the equation in

terms of a particular experimental procedure. For future reference equation (17b) is rewritten, using the definition of S from equation (18) and substituting T_1 for $1/2w$:

$$(19) \quad (a + b)/a = (S + j\omega ST_1)/(1 + j\omega ST_1).$$

4. EXPERIMENTAL PROCEDURE

The spectrometer, described more fully in Section 8, is of the bridge type with a heterodyne receiver. The receiver is linear over the whole range of signal levels employed. The microwave power level can be adjusted by variable attenuators between the oscillator and the bridge element. The audio-frequency signal from the linear detector of the I.F. system is fed via attenuators to an amplifier and phase-sensitive detector. The audio system is linear over the whole range of operation.

Consider that the d-c. magnetic field is set at a particular value somewhere near the center of the absorption line and that the bridge is adjusted so as to be sensitive to the imaginary component of the incremental susceptibility, $d\chi''$ (Feher 1957). The magnetic field is modulated over an amplitude range that is small compared to the linewidth, and the frequency is chosen from one of the several fixed audio frequencies for which the narrow-band amplifier is designed.

The microwave power is first set to a very low level so that saturation effects are negligible. The phase-sensitive detector and recorder are adjusted to give a good deflection, it being understood that any phase shift in the modulation coils and in the audio system can be balanced out.

The microwave power is increased by a definite amount, say 10 dB, by means of the microwave attenuators. If saturation is still negligible, an increase in the audio attenuation of 10 dB will leave the deflection unaltered. But if saturation is starting to become apparent, the deflection will be less and the phase-sensitive detector may show that the phase of the audio-frequency signal has been altered by a measurable amount. Several measurements can be made at different power levels, and at other modulation frequencies, to determine the effect of power level and modulation frequency on the phase and magnitude of the output signal. It should be noted that the use of a square-law detector in place of the heterodyne receiver would alter the procedure only to the extent that for each 10-dB decrease in microwave attenuation there should be a 20-dB increase in audio attenuation in order to maintain the same output signal, in the absence of saturation. Also, although we continue to discuss the procedure for the condition of a fixed value of the d-c. magnetic field, in practice the field is swept slowly through the line, and the signal intensities at corresponding points, that is, points equally distant from the center, are compared for various power levels and modulation frequencies.

In a spectrometer employing a heterodyne receiver the amplitude of the signal is proportional to the incremental power absorbed in the sample (Feher 1957). If n is the population difference between the two levels, the power absorbed per unit volume of the sample is given by $h\nu nV$. Writing n and V in terms of their average and fluctuating components, we obtain

$$P = h\nu\bar{n}\bar{V}(1 + ae^{j\omega t})(1 + be^{j\omega t}).$$

If the second-harmonic term is neglected, the incremental power dP can be written as

$$dP = h\nu\bar{n}\bar{V}(a + b)e^{j\omega t}.$$

We can substitute for \bar{n} the product Sn_0 . \bar{V} can be replaced by $JH_1^2\bar{g}(H)$, where $\bar{g}(H)$ is the average value of $g(H)$ over the modulation cycle. Therefore,

$$dP = h\nu n_0 J\bar{g}(H)H_1^2 S(a + b)e^{j\omega t}.$$

The microwave field H_1 is proportional to the square root of the input power. Therefore, according to the procedure outlined above, the relative signal from the phase-sensitive detector is proportional to dP/H_1^2 , which is given by

$$(20) \quad dP/H_1^2 = [h\nu n_0 J\bar{g}(H)]S(a + b)e^{j\omega t}.$$

When the input power level is low enough for saturation effects to be negligible, we have that $S \rightarrow 1$ and n is effectively constant. Hence $b \rightarrow 0$ as $S \rightarrow 1$, and the term $(a + b) \rightarrow a$. This unsaturated condition corresponds to maximum relative signal strength.

As the input power is increased, the saturation factor S decreases from unity and $(a + b)$ changes in magnitude and phase. From equation (20) the effect of saturation on the relative signal strength is determined by the product $S(a + b)$. If we use the symbol A to denote the relative signal strength when the system is partially saturated to that when $S = 1$, we have

$$(21) \quad A = [S(a + b)]/a.$$

Making use of equation (19), the dispersion equation becomes

$$(22) \quad A = S(S + j\omega ST_1)/(1 + j\omega ST_1).$$

Letting $A = A' + jA''$, and $\tan \theta = A''/A'$, we obtain

$$(23) \quad A' = S(S + \omega^2 S^2 T_1^2)/(1 + \omega^2 S^2 T_1^2),$$

$$(24) \quad A'' = \omega S^2 T_1(1 - S)/(1 + \omega^2 S^2 T_1^2),$$

$$(25) \quad \tan \theta = \omega ST_1(1 - S)/(S + \omega^2 S^2 T_1^2).$$

For a particular value of S the real and imaginary components of A change with frequency in much the same way as observed for other relaxation phenomena. From the form of the expressions it is apparent that the relaxation time T is equal to ST_1 , in agreement with derivations by Bloembergen *et al.* (1959) and Andrew (1956).

A' , A'' , and $\tan \theta$ are measurable quantities. Using two of the above equations, and knowing ω , it is possible to deduce values of both S and T_1 . But since the equations are not linear in T_1 , there is possible ambiguity in the reduction of data. In this respect it is instructive to interpret the dispersion in terms of a Cole-Cole diagram, as is often done for dielectrics (Cole and Cole 1941).

5. COLE-COLE DISPERSION DIAGRAM

With the substitution of τ for ST_1 in equation (22) a simpler form of the dispersion equation is obtained:

$$A = S(S + j\omega\tau)/(1 + j\omega\tau).$$

By rearrangement,

$$(26) \quad (S - S^2) = (S - A) + j\omega\tau(S - A).$$

The amplitude A is plotted in the complex plane in terms of its real and imaginary components A' and A'' in Fig. 4. If only ω is allowed to vary,

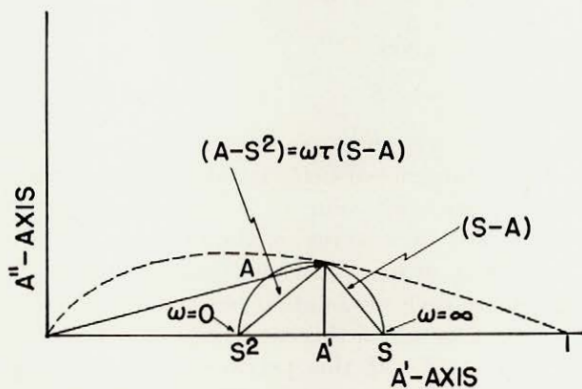


FIG. 4. Cole-Cole diagram for relative signal amplitude when saturation is present. The effective relaxation time τ is ST_1 .

equation (26) shows that the locus of A must cross the A' axis at $A' = S$ and $A' = S^2$, when $\omega = \infty$ and $\omega = 0$, respectively. According to equation (26), $(S - A)$ and $\omega\tau(S - A)$ are at right angles and add vectorially to equal $(S - S^2)$. Therefore, the locus of A must be a semicircle, and $(A - S^2)$ is equal to $\omega\tau(S - A)$.

There is one semicircle for each value of S , and so a whole family of semicircles can be drawn to include all values of S . As S approaches either of its limiting values, 0 or ∞ , the semicircle diameter $\rightarrow 0$. The maximum diameter is 0.25 and occurs for $S = 0.5$.

Ideally one might choose to set the power level, which in turn fixes S , and then take several determinations of A as ω is varied through the region of dispersion. But it is difficult to follow this experimental procedure since narrow-band amplifiers are required and the phase adjustments are sensitive to frequency. Measurements are therefore made at one modulation frequency for several levels of input power; then the frequency is altered and the process is repeated.

For a particular value of the modulation frequency the locus of A is constrained to lie only within the region represented by the family of semicircles. The path followed by A as S is varied depends primarily on the value of ωT_1 . If $\omega T_1 \gg 1$, the path is along the A' axis until very small values of S are

obtained. For example, if $\omega T_1 \simeq 10$, the phase angle θ is approximately 45° when $S = 0.1$. The modulation frequencies are therefore chosen so that measurable phase shifts occur when S is somewhere within the range 0.5–0.01.

6. REDUCTION OF DATA

The Cole–Cole diagram provides a simple means for reexpressing the information contained in equations (23), (24), and (25). Both S and T_1 have to be derived from the measured quantities A' , A'' , and $\tan \theta$, and it is important to remove ambiguity in the calculated results as far as possible.

The angle between $(S - A)$ and $(A - S^2)$ is 90° , and therefore

$$(27) \quad (A'')^2 = (S - A')(A' - S^2).$$

Substituting $A' \tan \theta$ for A'' gives

$$(28) \quad S^3 - A'S^2 - A'S + (A')^2(1 + \tan^2\theta) = 0.$$

Since equation (28) is cubic in S , there are three roots. Of these one is negative and can be neglected. The presence of two allowable solutions for S follows from the observation that a measured value of A can correspond to two of the Cole–Cole semicircles. If θ is close to the maximum angle permitted for A , the two solutions for S are very nearly equal and it is difficult to decide which is the correct one. Hence, for each modulation frequency it is advisable to keep the power level below that for which this condition can arise. A useful criterion is that $\omega\tau > 1$, or $S > 1/\omega T_1$. If this precaution is observed, the correct solution for S is the smaller of the two allowable roots of equation (28).

The method of successive approximations is a simple means for finding the roots of equation (28). The equation is quoted in two other forms, equations (29a) and (29b), which lend themselves to this approach:

$$(29a) \quad S = A' \left[1 + \frac{A'}{A' - S^2} \tan^2\theta \right],$$

$$(29b) \quad S = \sqrt{A'} \left[1 - \frac{A'}{S - A'} \tan^2\theta \right]^{\frac{1}{2}}.$$

For the first approximation, one sets $S = A'$ in the right-hand side of equation (29a) and calculates the approximate value of S from the experimental figures for A' and $\tan \theta$. This approximate S value is then used in the right side of the equation and a more accurate calculation made. The process can be repeated as often as warranted by the accuracy of the experimental data. This procedure, using equation (29a), leads to the lower of the two allowable roots, while a similar approach using equation (29b) leads to the higher of the two solutions. In using equation (29b) one substitutes $\sqrt{A'}$ for S in the right side of the equation for the first approximate calculation. The approximate relations corresponding to equations (29a) and (29b) are given in equations (30a) and (30b), respectively:

$$(30a) \quad S \approx A' \left(1 + \frac{\tan^2\theta}{1 - A'} \right),$$

$$(30b) \quad S \approx \sqrt{A'} \left(1 - \frac{\sqrt{A'}}{1 - \sqrt{A'}} \tan^2 \theta \right)^{\frac{1}{2}}$$

One further set of equations is necessary for calculating T_1 from the data on A' ; $\tan \theta$, S , and ω . In the Cole-Cole diagram $(A - S^2) = \omega\tau(S - A)$; hence, from similar triangles,

$$\frac{\omega\tau(S - A)}{S - A} = \frac{(A' - S^2)}{A''}$$

Putting $A'' = A' \tan \theta$, and $\tau = ST_1$, we have

$$(31a) \quad T_1 = \frac{(A' - S^2)}{A' S \omega \tan \theta}$$

An equivalent expression can also be derived:

$$(31b) \quad T_1 = \frac{A' \tan \theta}{S \omega (S - A')}$$

Both equations, (31a) and (31b), should give the same answer for T_1 . But small experimental inaccuracies can lead to fairly large errors in T_1 because of the difference in term $(A' - S^2)$ or $(S - A')$. If the magnitude of A' is closer to S than to S^2 , then equation (31a) should be used. This will be the case if $\omega\tau > 1$.

In all experimental work reported here $\omega T_1 > 1$. Under these circumstances the power is increased until θ is about 45° , and the data are reduced by equations (30a), (29a), and (31a).

When $\omega T_1 \approx 1$ it should be possible to employ a different approach. Using equation (25), we find by differentiating the numerator and denominator that $\tan \theta \rightarrow \omega T_1$ as $S \rightarrow 0$. When $\omega T_1 \gg 1$, this limit is approached only when S is very small, but if $\omega T_1 = 1$, the value of $\tan \theta$ should be within 10% of its limiting value when $S = 0.05$.

7. EQUIVALENT CIRCUIT

Equations (17) to (25) can be interpreted in terms of an equivalent circuit shown in Fig. 5. The choice of parameters to correspond with voltage is somewhat arbitrary, but the circuit as illustrated has been found to be helpful.

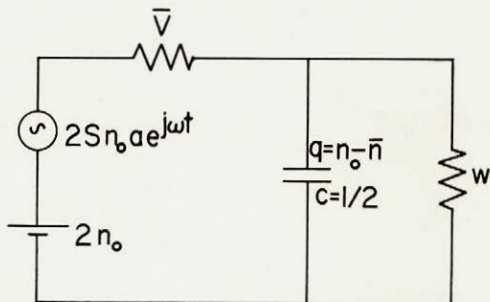


FIG. 5. Equivalent circuit of a two-level system. The mean saturation factor is obtained from the fractional d-c. voltage across \bar{V} , and the relative a-c. signal can be calculated from the a-c. voltage across \bar{V} .

Equation (17a), which gives the mean value of the population difference, \bar{n} , in terms of \bar{V} , w , and n_0 , can be considered to correspond to the d-c. circuit. The relaxation path is by way of the spin-lattice probability w , and the relaxation process is equivalent to a RC discharge. The capacitance value should be $\frac{1}{2}$ in order to have the correct relaxation time $T_1 = 1/2w$. The equivalent charge should be proportional to the amount by which the population is disturbed from the equilibrium value, and if we take q as equal to $(n_0 - \bar{n})$ the remainder of the d-c. circuit is determined; that is, the voltage across the capacitor is $2(n_0 - \bar{n})$, the e.m.f. is $2n_0$, and the voltage across \bar{V} is $2\bar{n}$. Incidentally, the microwave power absorbed in the sample is proportional to the equivalent current $2\bar{n}\bar{V}$. The current has dimensions of dn/dt , and equation (17a) expresses the fact that the average current flowing into the capacitance is zero because the radiation-induced rate of change of population is balanced by the relaxation rate. The saturation factor \bar{n}/n_0 is given by the ratio of the voltage across \bar{V} to the source voltage.

The dispersion relationship expressed by equation (17b) is also described by the same basic RC circuit, with the addition of an a-c. source voltage. The incremental voltage across \bar{V} increases when the modulation frequency is made to increase, resulting in a signal at very high frequencies $1/S$ times the low-frequency value. Equation (17b) can be interpreted as showing that the net a-c. current at the junction point of \bar{V} , w , and C is zero. If we drop the frequency factor $e^{j\omega t}$, the current flowing through \bar{V} equals $2\bar{n}\bar{V}(a+b)$, the component through w is $2\bar{n}b\omega$, and that through the capacitance is $j\omega\bar{n}b$. If a is taken as a positive real number, then it is necessary for b to be complex, with the real part negative and the imaginary part positive. The a-c. voltage across the capacitance is given by $-2\bar{n}b$, that across \bar{V} is $2\bar{n}(a+b)$, and the source voltage must equal $2\bar{n}a$, or $2Sn_0a$.

A slightly different version of the circuit for a two-level system is shown in Fig. 6. It appears obvious that one should be able to extend this circuit to include multilevel systems by placing a capacitor between each node of the mesh and the neutral point, but theoretical justification for this has not yet been established for more than the two-level system.

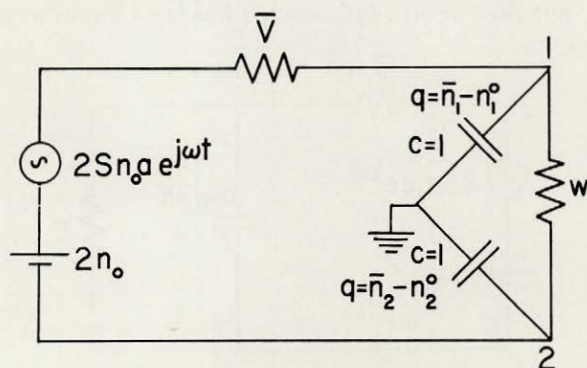


FIG. 6. Modified equivalent circuit which has a capacitor from each node to a neutral point.

8. APPARATUS

Figure 7 shows a block diagram of the spectrometer which is patterned after apparatus described by Feher (1957). The superheterodyne receiver is linear

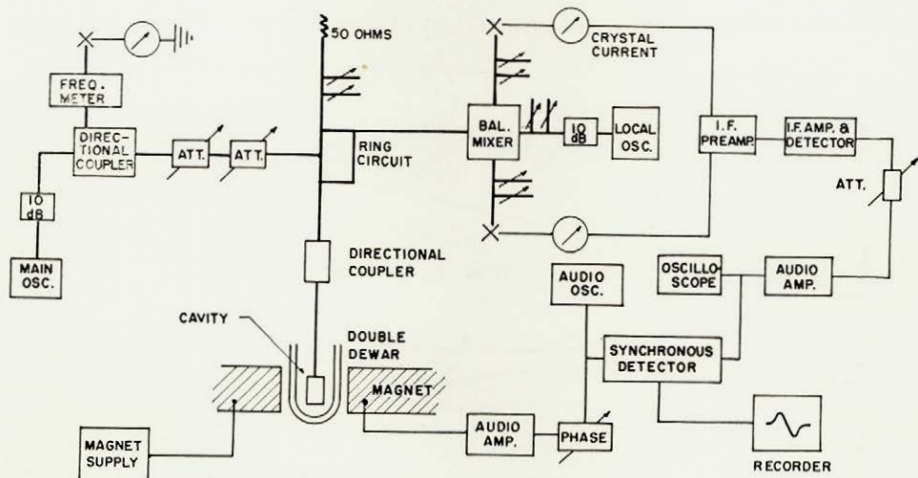


FIG. 7. Block diagram of the spectrometer.

over the signal range used in the experiment. The bridge element is a coaxial ring circuit built from modified General Radio 874 components. The balanced detector is based on a GR 1602B admittance bridge modified by increasing the coupling between the "detector" arm and the "load" arms to give adequate crystal currents from the local oscillator coupled into the "detector" arm. The 1209B main oscillator is free running and has been provided with good temperature lagging and sound insulation. Well-regulated d-c. supplies are used for the filament and H.T. currents. In the receiver a balanced I.F.I. P205 preamplifier is followed by a GR 1216A I.F. amplifier which has one stage bypassed and the bandwidth increased from the factory setting. The audio amplifier uses plug-in twin-T elements to provide narrow-band response at the audio frequencies used, i.e. 35, 140, 400 c/s. A Phazor 200A phase-sensitive detector drives a Texas Servoriter recorder of 5-mV full-scale sensitivity. A conventional phase-shifting circuit using an RC load on a center-tapped transformer, is placed in the line to the modulating coils to control the phase of the modulating field.

9. EXPERIMENTAL CONDITIONS

Crystals of dilute $K_3Cr(CN)_6$ were grown in the laboratory from solutions of paramagnetic $K_3Cr(CN)_6$ and diamagnetic $K_3Co(CN)_6$. Concentrations of the Cr^{3+} ion were measured by the method of Sandell (1959) and found to be about one half of the nominal concentration. The two concentrations used for these experiments were 0.1% and 1.0% nominal, 0.06% and 0.4% measured.

Tables of the energy-level structure of potassium chromicyanide have been published by Chang and Siegman (1958), and several graphs are given by Butcher (1957). Most of the data reported here are for a crystal orientation which places the z axis of one magnetic complex parallel to the static magnetic field. The four transitions are indicated in Fig. 8. Actually there are six lines, because the other magnetic complex gives additional lines at 100 and 300 gauss.

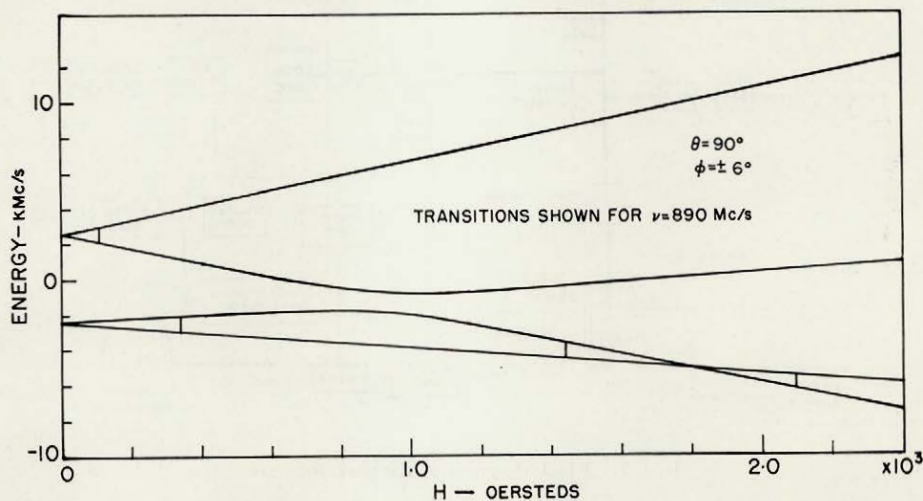


FIG. 8. Energy level diagram for $K_3Cr(CN)_6$ for H parallel to the z axis. The four transitions at 890 Mc/s occur for 100, 300, 1 400, and 2 100 oerstedes.

Since the two 100-gauss lines are not properly resolved, some of the data for the 100- and 300-gauss lines were taken with the crystal rotated 6° in the ab plane, so that the static magnetic field and the a axis of the crystal were parallel. In this case the energy levels for the two complexes are superimposed and single lines are observed at 100 and 300 gauss. Comparison of data for the 300-gauss lines did not show a measurable difference in the value of T_1 for the two orientations.

All measurements were made at $4.2^\circ K$ with the crystals in contact with the liquid helium. The microwave operating frequency was 890 mc/s. The amplitude of modulation was maintained at a low level to ensure that the line shape did not depend on the modulation amplitude.

10. RESULTS

The 300-gauss line was studied more intensively than the others because of the better signal-to-noise ratio. Data were obtained at three audio modulation frequencies and for each of the two orientations. These results are summarized in Fig. 9, where the observed values of T_1 are plotted as a function of the saturation factor S . The fact that the points are grouped into lines with finite slope is an indication that the relaxation system does not have a unique time-constant.

The results for the lower concentration (0.06%) lie along a line of much lower slope than those for the higher concentration, and it is more meaningful

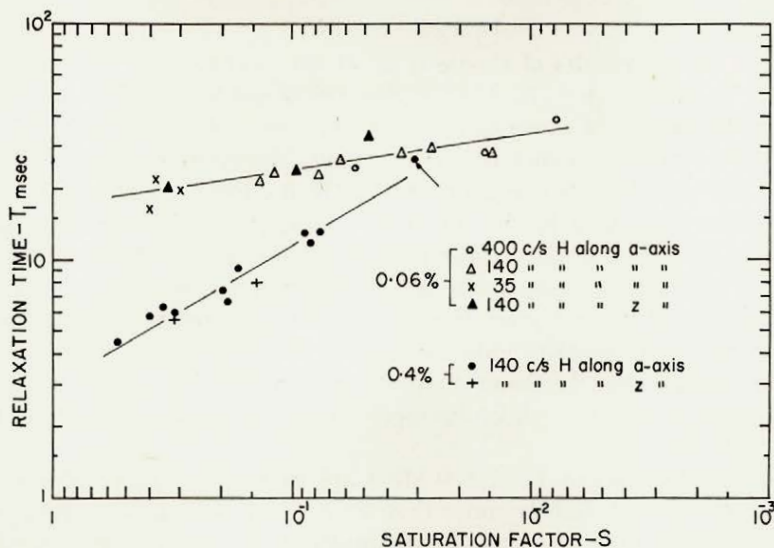


FIG. 9. Relaxation times at 890 Mc/s and 300 oersteds for dilute $K_3Cr(CN)_6$ crystals. The dependence of T_1 on the saturation factor indicates that relaxation cannot be represented by a single time-constant.

to speak of the effective lattice relaxation time T_1 . The question still arises as to which value should be picked from the graph, and in this respect the data do not give as clear a picture as would be obtained from results using the pulse technique. It is seen that the lines for the two concentrations cross, and it is presumed that for lower concentration of the Cr^{3+} ion the results would lie along a line with less slope and would again cross the other two. For this reason, and others discussed in the next section, it is considered that the best value of T_1 is about 30 milliseconds.

For comparison of T_1 for the four different lines several results have been averaged with S between 0.25 and 0.1, measured with $\omega_m = 35$ c/s. Note that the data in Fig. 9 do not indicate significant differences for the two crystal orientations. The averages of Table I were obtained by using only data for the

TABLE I
Spin-lattice relaxation time T_1 in 0.06%
crystals of $K_3Cr(CN)_6$ for four lines at
890 Mc/s

H_0 (oersteds)	T_1 (milliseconds)
100	22
300	23
1 400	24
2 200	29

0.06% crystals. Poor signal-to-noise ratios were observed for the high field lines and it was not feasible to work at small values for S . Similar comparisons were obtained for the higher concentration, 0.4%.

11. DISCUSSION

From the x -band results of Castle *et al.* (1960) and Kipling *et al.* (1961) it was expected that single-valued relaxation times would be observed at concentrations below 1%. Failure to observe this even at 0.06% shows the need for further studies. Although Castle *et al.* (1960) observed an inverse temperature dependence of T_1 at temperatures of 4.2 °K and lower, there was a suggestion of a changeover to a Raman process at temperatures only a little above 4.2 °K. From this, one might expect that the results reported here, at 4.2 °K and 890 Mc/s, do not correspond to a "direct" process and are therefore not comparable with those at x band. Further work in this area is now in progress, and preliminary data seem to indicate that for the 300- and 1 400-gauss lines at least, T_1 varies slightly faster than the reciprocal of the temperature at 4.2 °K, suggesting that the relaxation mechanism is in a transition region from the Raman to the direct.

The measured values of T_1 at 890 Mc/s are longer than those observed at x band by a factor of slightly more than 3. But calculations currently being worked out, which take into account the multiple relaxation paths present in the system, yield results for the average relaxation times at 890 and 9 400 Mc/s which are in fair agreement with measurements. The results of these calculations, when completed, will be published separately.

The extent of the variation of T_1 with S was found to depend on the concentration, much as the appearance of multiple time-constants in x -band pulse measurements at higher concentrations. Although the presence of several relaxation paths can obviously result in multiple time-constants, this effect should not be dependent on the concentration. Furthermore, one should observe a different dependence of T_1 on S for each of the modulation frequencies, an effect which did not show up in the measurements. Therefore, it appears necessary to look for some other mechanism to account for the variation of T_1 with S . Cross relaxation between pairs of levels is not expected to be observable at the crystal orientations used. However, cross relaxation via excited states along the lines suggested by the work of Gill and Elliot (1961) and Bloembergen and Pershan (1961) is suggested as a possible explanation. Further experiments at different concentrations and orientations are indicated in order to clarify this aspect.

ACKNOWLEDGMENTS

The authors gratefully acknowledge the support given to this research by the Defence Research Board, through grant DRB 9512-20. One of us (N. C. R.) wishes to acknowledge research grants from the Scientific Research Bureau of the Province of Quebec. Throughout the research, the help in the construction of equipment provided for us by Mr. V. Avarlaid and his assistants has been invaluable.

REFERENCES

- ANDREW, E. R. 1956. Nuclear magnetic resonance (Cambridge University Press, London and New York).
BLOEMBERGEN, N. and PERSHAN, P. S. 1961. Advances in quantum electronics, *edited by* Jay R. Singer (Columbia University Press, London and New York), p. 373.

- BLOEMBERGEN, N., PURCELL, E. M., and POUND, R. V. 1948. *Phys. Rev.* **73**, 679.
- BLOEMBERGEN, N., SHAPIRO, S., PERSHAN, P. S., and ARTMAN, S. O. 1959. *Phys. Rev.* **114**, 445.
- BUTCHER, P. N. 1957. Electron Tube Laboratory, Tech. Rept. No. 155-1, Stanford Electronics Labs., Stanford, California.
- CASTLE, J. G., CHESTER, P. F., and WAGNER, P. E. 1960. *Phys. Rev.* **119**, 953.
- CHANG, W. S. and SIEGMAN, A. E. 1958. Electron Tube Laboratory Tech. Rept. No. 156-1, Stanford Electronics Labs., Stanford, California.
- COLE, K. S. and COLE, R. H. 1941. *J. Chem. Phys.* **9**, 341.
- FEHER, G. 1957. *Bell System Tech. J.* **36**, 449.
- GILL, J. C. and ELLIOT, R. J. 1961. *Advances in quantum electronics*, edited by Jay R. Singer (Columbia University Press, London and New York), p. 399.
- GORTER, C. J. 1947. *Paramagnetic relaxation* (Elsevier Publishing Company Inc., Amsterdam).
- KIPLING, A. L., SMITH, P. W., VANIER, J., and WOONTON, G. A. 1961. *Can. J. Phys.* **39**, 1859.
- LLOYD, J. P. and PAKE, G. E. 1954. *Phys. Rev.* **94**, 579.
- PAXMAN, D. H. 1960. Rept. No. 364, Mullard Research Labs.
- SANDELL, E. B. 1959. *Colorimetric determination of traces of metals* (Interscience Publishers Inc., N.Y.).
- VAN VLECK, J. H. 1960. *Quantum electronics*, edited by C. H. Townes (Columbia University Press, N.Y.), p. 392.
- 1961. *Advances in quantum electronics*, edited by Jay R. Singer (Columbia University Press, London and New York), p. 388.
- WALLER, I. 1932. *Z. Physik*, **79**, 370.

